Final report: Population assessment of Smalleye (*Notropis buccula*) and Sharpnose (*Notropis oxyrhynchus*) shiners in the Brazos River and data-driven recommendations for long-term monitoring

Submitted by Dr. David Hoeinghaus (PI), on behalf of all investigators
David.Hoeinghaus@unt.edu

The goals for this research were to 1) develop a long-term ecological monitoring program for the assessment of Sharpnose and Smalleye shiner populations and associated fish assemblages, their habitat use, and the quality of habitats used by different life stages, 2) improve understanding of the environmental factors (abiotic and biotic) affecting Sharpnose and Smalleye shiner population distributions and dynamics, 3) make recommendations to conservation professionals and other stakeholders based on findings that can inform conservation actions for the focal species at appropriate spatial and temporal scales, and 4) work with transparency to provide methodologies, data and results to stakeholders and diverse end-users in a variety of formats. Finally, we make data-informed recommendations regarding the design of a long-term monitoring program, such as sampling period, frequency and method(s) to optimize long-term monitoring efforts for Sharpnose and Smalleye shiners.

Task 1: Agency will review recent research related to project objectives and coordinate with other researchers

The Sharpnose Shiner (*Notropis oxyrhynchus*) and Smalleye Shiner (*Notropis buccula*) are two species of small cyprinids endemic to the Brazos River, Texas, historically occurring throughout the mainstem Brazos River (Cross 1953, Moss and Mayes 1993). The Sharpnose Shiner also used to naturally occur in the headwater of the Red River and Colorado River basins within the semi-arid High Plains ecoregion, but surveys in these rivers have not yielded individuals of this species since the 1960s. As a recently as 1991, Sharpnose Shiner was collected in the lower Brazos River downstream from Marlin, Texas (Moss and Mayes 1993, Gelwick and Li 2002). However, later surveys in 2000 and 2001 did not include specimens of the Sharpnose Shiner throughout the lower Brazos suggesting a population decline (Gene Wilde, unpublished data). Also, Zeug et al. (2005) reported catches of Smalleye Shiner in oxbow lakes of the lower Brazos, but subsequent surveys did not collect this species. Studies of the fish assemblages of the Brazos River suggest that these two shiners still occur in the Brazos River but are limited to segments upstream of Possum Kingdom Reservoir (Ostrand 2000, Wilde and Durham 2008, USFWS 2014, Wilde 2015). Both Sharpnose and Smalleye shiners have been species of conservation concern since 1982 and in 2014 were federally listed as endangered species because of population declines due to habitat modifications (USFWS 2014).

Modification of the upper (portion of the basin upstream Possum Kingdom Reservoir) and middle (portion between downstream Possum Kingdom and Lake Waco) Brazos River with construction of dams have heavily affected the flow regime resulting in loss of prairie stream habitat for several native species including the Sharpnose and Smalleye shiners (Anderson et al. 1983, Moss and Mayes 1993, Wilde and Ostrand 1999). Portions of the upper Brazos River are also affected by fish passage barriers, the introduction of nonnative fish and plant species, and the discharge of treated domestic and wastewater effluents (USFWS 2014, Wilde 2015, Mayes et al. 2019, Kelly and Wilde 2020). The introduction of saltcedar (*Tamarix* sp.) in the upper Brazos River basin has resulted in dramatic changes in the riverscape, as this invasive tree species has expanded and is present in high densities along the river edges (Wilde 2018). The invasion of saltcedar appears to be responsible for high flood stages, sediment accumulation, and reduction of the Brazos River's width (Wilde 2018, Mayes et al. 2019). Collectively, these ongoing impacts in the upper Brazos River have altered the habitat for fishes adapted to the stream's natural geomorphology and water chemistry (Perkin et al. 2015, Mayes et al. 2019).

The fish fauna in the upper Brazos River is primarily dominated by five species: Red shiner (*Cyprinella lutrensis*), Plains minnow (*Hybognathus placitus*), the threatened species Red River pupfish (*Cyprinodon rubrofluviatilis*), and Smalleye and Sharpnose shiners (Wilde 2015, Montaña unpublished data). Also, the western mosquito fish (*Gambusia affinis)* and Shoal chub (*Macrhybopsis hyostoma)* appear common in some segments of the upper Brazos River. The Plains minnow, Shoal chub, and Smalleye and Sharpnose shiners are members of the reproductive guild of pelagic broadcast-spawning cyprinids with external fertilization, which are common in Great Plains rivers (Hoagstrom and Turner 2013). Flowing water is essential for successful reproduction, survival of eggs and larval fish of this reproductive guild (Platania and Altenbach 1998, Durham and Wilde 2009, Wilde 2015). In pelagic broadcast-spawners, eggs and sperm are released into the water column where fertilization subsequently occurs (Platania and Altenbach 1998, Hoagstrom and Turner 2013). Flowing water will allow the ova and newly hatched fry stay suspended by the current, preventing them from settling to the river bottom

where they may be covered and suffocated with sand, sediments and silt (Platania and Altenbach 1998). Based on studies of cyprinids with a similar reproductive guild (e.g., Arkansas River shiners, *N. Girardi* [Moore 1944]), minnows/shiners (cyprinids) eggs spawned into the open water column become semi-buoyant within 10-30 minutes and drift through the water column for about 72 to 144 km downstream for one to two days prior to hatching (Moore 1944, Platania and Altenbach 1998). For pelagic broadcast-spawning Brazos River shiners (e.g. Sharpnose and Smalleye shiners), it has been estimated that relatively long (~275 km), unobstructed river segments are required for reproduction, hatching and larval development of these two species in the upper Brazos River (Wilde and Urbanczyk 2013, USFWS 2015).

Studies in their ecology and life history suggest that Smalleye and Sharpnose shiners are generalist feeders that spawn continuously during their reproductive season, a strategy that has been linked with stochastic environments to ensure survival of the offspring (Marks 1999, Durham 2007). These two shiners appear to have a maximum life span of less than three years (Marks 1999). Early life stages (eggs and larvae) of these species are susceptible to predation and adverse environmental conditions, resulting in low survival of age-0 fish (Durham 2007; Durham and Wilde 2009). Durham and Wilde (2009) suggest that the two Brazos River shiners have asynchronized spawning from April through September during periods of low or no-flow, while large synchronized spawning event occur during high stream flow events. These authors also suggest that during periods of low flow, successful survival to juvenile stages does not occur. While the Sharpnose and Smalleye are physiologically tolerant of naturally and abiotically variable conditions typical of High Great Plain streams, the increase of anthropogenic changes in the river – such as altered water chemistry due to wastewater and industrial pollutants, sedimentation, habitat fragmentation, and flow alteration – pose a critical threat to the survival of both shiners. These ongoing impacts and the severe drought of two consecutive years (2011-2012) raised concerns about the potential extinction of these species within the reduced distribution segments in the upper Brazos River, a reason that led the USFWS to list these two species as endangered in 2014 and identified most segments of the Brazos River (as suggested by Moss and Mayes 1993, Durham 2007, and Wilde 2015) as critical habitats for survival and persistence of these shiners (USFWS 2014, 2015). During the 2011 drought, there was not documentation of reproduction of the Sharpnose and Smalleye shiners, perhaps attributed to the severe reduction of the river flow. However, surveys in 2012 suggested successful recruitment of these two shiners, suggesting that these species are resilient to warmer stream temperatures and drier conditions observed during these years (USFWS 2014).

The comprehensive report presented by USFWS in 2018 "Species Status Assessment for the Sharpnose Shiner (*Notropis oxyrhynchus*) and Smalleye Shiner (*N. buccula*) Version 2" (USFWS 2018), which accounted for the species' resource needs, threats, current conditions, and projected future conditions, suggested that because of the life history requirements and short life span of these two shiners, there is a low probability of persistence (i.e. low viability) in the near term (next 10 years) of the populations in the upper Brazos River, which is attributed to substantial changes in river flows induced by human use and drought-enhanced water shortages. Furthermore, this report highlights that the contiguous stretches of river where extant shiner populations are currently found appear suitable and long enough to support recruitment, suggesting that these species can be resilient to local stretches with short-term environmental changes (USFWS 2018). In 2020, USFWS presented a draft Recovery Plan for the Sharpnose and Smalleye shiners which intended to provide a vision (based on resilience and viability of focal species), strategy (restoring and management of unit where the populations occur), and

criteria (review species' status) to recover these two endangered species (USFWS 2020). Given the perceived threats affecting these two endangered species, all of which are expected to continue or increase over time, long-term monitoring is needed to understand and ultimately forecast population responses to changing environmental conditions and promote recovery of both species (USFWS 2014).

Previous research in this study system, including the studies cited above, relied on standardized seine surveys to characterize the distribution and relative abundances of stream fishes including the focal Sharpnose and Smalleye shiners. In general, standardized seining is recognized as highly effective for surveying fishes in wadable streams, which is why it is included in standard field methods in Texas and elsewhere (e.g. TCEQ 2014). No previous studies directly compared results from seining with passive sampling techniques like fyke nets or minnow traps, and environmental DNA (eDNA) approaches and passive integrated transponder (PIT) tagging had not been used for Sharpnose and Smalleye shiners prior to this project.

Throughout this research project, we coordinated with agency and university partners working in the Upper Brazos River system. This includes Kevin Conway and Josh Perkin at Texas A&M University, and David Portnoy at Texas A&M University – Corpus Christi. In particular, David Portnoy and Kevin Conway were able to provide mitogenomes for the focal species and other taxa needed for primer development (described below), at a cost savings to this project. Kevin Conway was instrumental in providing tissues from specimens vouchered in the Texas Cooperative Wildlife Collection for primer development and testing. Agency personnel were helpful with permitting and assistance throughout.

Task 2: Agency will evaluate the efficacy of current, existing and alternative (traditional and non-traditional) survey protocols to accurately estimate population parameters of Smalleye and Sharpnose Shiners.

Field surveys were conducted at 22 sites in the Upper Brazos River basin (UBRB) upstream of Possum Kingdom Reservoir (Figure 1). The study area corresponds with segments of the upper Brazos River where Sharpnose and Smalleye shiners are currently restricted, including the Salt Fork (SF), Double Mountain Fork (DMF) and the Brazos River mainstem (BRM; Figure 1). The headwaters of the UBRB are primarily comprised by ephemeral streams that, when flowing, deposit into the SF and DMF, providing dynamic habitat with rapidly changing physical and chemical conditions (Baldys and Schalla 2012; Mayes et al. 2019; Ostrand and Wilde 2002). Landscape and vegetation are heterogenous throughout the UBRB with scrub and shrub dominating the landscape, ranchland used for livestock, and little canopy coverage. Lower portions of the basin, while having more riparian tree coverage and vegetation, also contain significant amounts of scrub and shrub along the river's banks and extensive agricultural land. The presence and expansion of invasive saltcedar (*Tamarix spp.*), a halophytic phreatophyte that can withstand inundation and quickly colonize moist farmland and riparian zones is an increasing concern in the UBRB (Auerbach et al. 2013; Brotherson and Field 1987; Mayes et al. 2019; Shafroth et al. 2005).

The start of monthly sampling was delayed due to extreme drought throughout the upper Brazos River basin during summer 2022. The research team was in regular contact with the Comptroller's Office (Jake Jackson) as well as state (TPWD: Megan Bean, Kevin Mayes), federal (USFWS: Omar Bocanegra), and university (e.g. TAMU: Josh Perkin) stakeholders with expertise in the focal species and the study system. The research team contributed to stakeholder

discussions and decision-making (e.g. regarding possible salvage sampling for refuge populations as done during the drought in 2011) by assessing conditions at field sites multiple times during the summer. Specific attention was paid to the availability of water, habitat fragmentation, and fish species present (including presence of dead Sharpnose and Smalleye shiners). We also mapped habitat availability and connectivity upstream and downstream of bridge crossings using drone surveys at each site during each visit. These data were shared with stakeholders prior to and during a meeting in August 2022. Research team members also participated in a TPWD-led collection of Sharpnose and Smalleye shiners in September 2022 to establish captive rearing populations at the USFWS Uvalde National Fish Hatchery. Although monthly sampling was delayed, we used that time to generate opportunistic data and refine some of the proposed methodologies. Specifically, water samples for eDNA analyses were collected wherever water was present during site visits in summer 2022. While collecting water samples, we tested a methodology for filtering water in the field, which if efficient would have reduced cost and storage volume in the truck. Unfortunately, we found that filtering water samples in the field was extremely time consuming due to turbidity and productivity of the system which results in clogged filters, thus we proceeded with the original plan of freezing water samples on dry ice and filtering in the lab. In the lab, we tested a newly developed DNA isolation kit (Qiagen

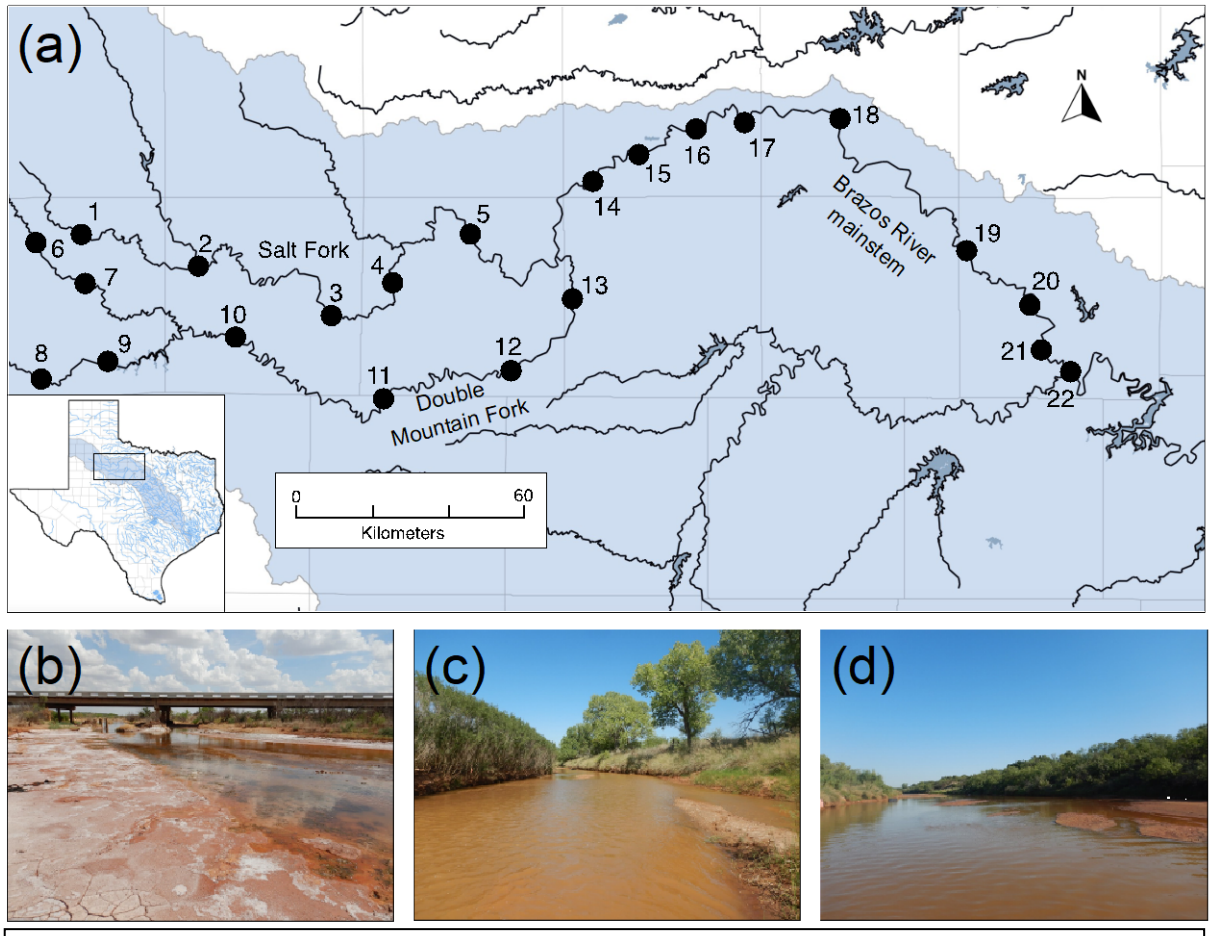


Figure 1: Spatial distribution of the 22 sampling sites along the river segments of the (a) upper Brazos River in Texas including the (b) Salt Fork (SF), (c) Double Mountain Fork (DMF) and the (d) Brazos River mainstem (BRM).

PowerWater) that was specifically developed for use with water samples and compared DNA yield from that kit with more traditional approaches. Our results indicated that the traditionally used DNA isolation kit performed better than the new water-specific kit, so we proceeded as originally planned. Both of these methodological findings are important for study design and logistics associated with eDNA biomonitoring in this, and similar, study systems.

Field surveys were conducted over three years at all sites. Monthly sampling was conducted at all sites during the first two years (September 2022 through August 2024) followed by quarterly/seasonal sampling during the third year of field surveys (Fall 2024 through Summer 2025). Field survey methods largely followed standard protocols for wadeable streams (TCEQ 2014), with additional components to meet study objectives. Specifically, five transects perpendicular to the stream were designated at each site, starting at least 20 m upstream of the bridge crossing right-of-way that was used to access the site. Transects were spaced 50 m apart, for a total surveyed stream reach of 200 m. Biological surveys were conducted with the 200 m stream reach, as described below, whereas environmental attributes were measured along each transect. Water depth (m), flow velocity (m/s), dissolved oxygen concentration (DO, mm/L), and temperature (degrees C) were measured at five equidistant points (left bank, left center, center, right center and right bank) along each transect. Turbidity (NTU), conductivity (μS/cm), and pH were measured once at each transect in the thalweg or center. Depth was measured using a marked depth pole, flow velocity was measured using a Marsh McBirney Flo-Mate 2000, DO, temperature and conductivity were measured using a YSI ProQuatro Multiparameter Meter, turbidity was measured using an Apera TN400 turbidity meter, and pH was measured using an Apera PH60 Pocket Meter. Wetted width was measured at each transect using either a metric field tape or a range finder (Bushnell Halo XL 450). Canopy coverage was quantified using a convex densiometer (Forestry Suppliers Model-A), quantified at four positions on each transect (at each bank facing the riparian zone, and at the center of the transect facing each bank). Percent coverage of woody debris, macrophytes, algae and saltcedar, along with percent undercut for each bank, were estimated for each transect. During each sampling event, aerial photographs were taken using an Autel Evo 2 drone, programmed to fly at a consistent height and capture imagery (multiple photographs) that covered the entire stream reach. Aerial photographs from each sampling event were overlayed to yield a single composite image covering the entire stream reach and used for estimating connectivity throughout the reach for each sampling event. Connectivity was quantified using $c = 1/(f + 1)$, where c is the connectivity index value, and f is the number of complete breaks in connectivity with the 200 m stream reach. Therefore, a fully connected stream reach, where f=0, has a value of c=1 and increasing degree of fragmentation (more breaks in connectivity) is represented by values of c closer to zero. Stream segments that are completely dry are assigned a value of c=0.0.

Following standard protocols (and analogous to previous studies in the Upper Brazos and other plains streams), fishes were sampled during all sampling events at all sites using a 3 x 1.5m seine with 4mm delta mesh. All available habitats within a reach were sampled using up to 10 non-overlapping seine hauls, with each haul approximately 10 m in length (some sites were sampled thoroughly with less than 10 seine hauls because they were mostly dry and only contained one or more small isolated pools). Collected individuals were held in clean buckets and/or coolers filled with aerated stream water until sampling was completed. In addition to seining, fishes were also sampled using conical minnow traps and mini-fyke nets (4mm delta mesh) at all sites during the first 10 months of the project. Fyke nets and minnow traps were deployed prior to seining and retrieved after all seining and quantification of environmental

parameters was completed. Regardless of sampling methodology, all collected individuals were identified, measured and returned to the stream following completion of surveys. In addition to the aforementioned traditional sampling methods, we also collected water samples for eDNA metabarcoding. Triplicate water samples for eDNA were collected prior to any other activity at the stream to avoid foreign DNA contamination. Water samples were collected using sterile 500mL bottles, from a downstream to upstream manner from the thalweg (primary flow path to maximize capture of suspended eDNA) at the 1st, 3rd, and 5th transect within each site, flash frozen on dry ice and stored at -80 °C for subsequent processing in the lab.

During the two years of monthly field sampling, 82,820 individuals were collected using standardized seining, representing 32 taxa. Of those, 13,444 Sharpnose Shiner were collected across 261 unique occurrences and 9,188 Smalleye Shiner were collected across 277 unique occurrences (out of a possible 528 occurrences: 22 sites x 24 months). When adding the four seasonal events following monthly sampling, total abundances for Sharpnose and Smalleye

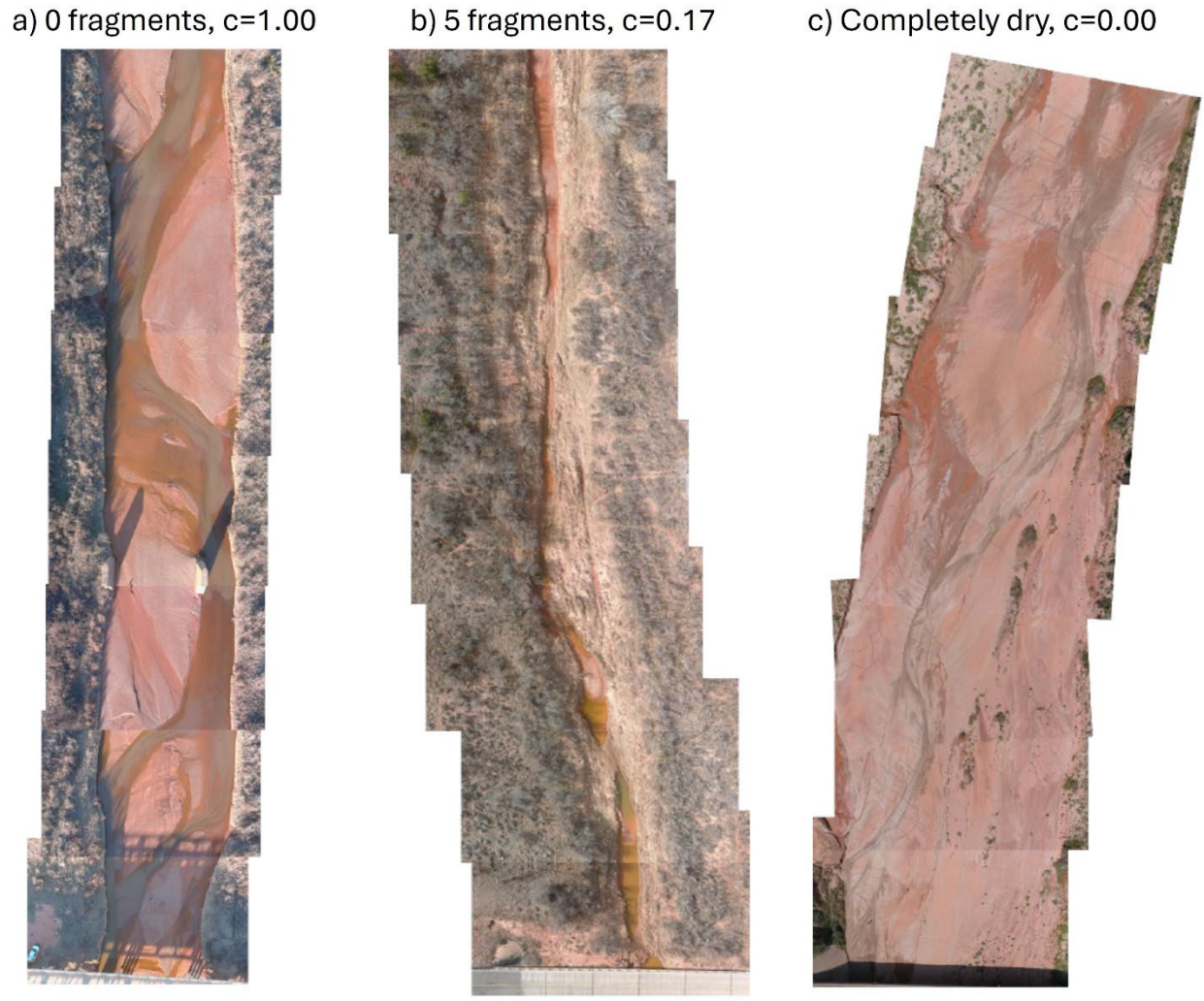


Figure 2: Examples of connectivity index determination using aerial photographs. Connectivity index values were quantified using c=1/(f + 1) where f is the number of fragments in connectivity. Sites that are completely dry are assigned a value of c=0.00. a) fully flowing, b) fragmented, c) dry.

shiners were 14,479 and 9,493, respectively. In total, across all study sites during the first ten sampling events, 44,210 individuals were collected using seines, whereas fyke nets caught 12,104 individuals, and minnow traps only caught 315 individuals. Furthermore, 28 of the 29 total species recorded during that period (not considering a few juvenile sunfish individuals registered as Lepomis spp.) were collected using seines. Smallmouth Buffalo were not collected during seining, and only 1 individual was collected using fyke nets in April 2023. In comparison, 23/29 species were collected using fyke nets and 10/29 were collected using minnow traps. Sampling with fyke nets was discontinued after June 2023 and sampling with minnow traps was discontinued following August 2023, with sponsor approval, due to logistical constraints and the fact that those gears only captured a subset of the species collected with standardized seining.

Using the first year of field data and standardized seining data, we assessed environmental and spatial determinants of fish assemblage structure and temporal dynamics. Non-metric multidimensional scaling (NMDS) was used to visualize differences in fish assemblage structure to assess the spatial variation of fish assemblages among river segments, as well as to evaluate the temporal variation of fish assemblages across time periods (i.e., bimonthly) within each river segment. NMDS was performed using a Bray-Curtis dissimilarity metric on Hellinger transformed assemblage data (Borcard et al. 2018). Permutational multivariate analysis of variance (PERMANOVA) with 999 permutations was used to test for significant differences in fish assemblage structure (among river segments or bimonth periods), and pairwise PERMANOVA with 10,000 permutations was used to assess pairwise differences in assemblage structure between river segments or bimonthly periods (Anderson 2001). NMDS, PERMANOVA and pairwise PERMANOVA were performed using the vegan package and "adonis2" function (Oksanen et al. 2022). Spatially, fish assemblages showed significant differences among the three river segments (PERMANOVA: Pseudo-F2 = 6.43, $p < 0.01$; Figure 3a). Results from pairwise PERMANOVA comparisons revealed significant differences in fish assemblages between the SF and the DMF (Pseudo-F11 = 4.67, $p = 0.02$), the SF and the BRM (Pseudo-F12 = 9.22, $p < 0.01$), and the DMF and the BRM (Pseudo-F15 = 5.43, $p < 0.01$) (Figure 3a). Temporally, pairwise PERMANOVA comparisons revealed significant differences in the assemblage from the January-February (janfeb) period and the July-August (julyaug) period in the BRM (PERMANOVA: Pseudo-F16 = 5.47, $p = 0.04$; Figure 3c), but neither the SF (Figure 3b) nor the DMF (Figure 3d) showed bimonthly changes.

Variance partitioning was used to evaluate the shared and unique contribution of time, space, and environmental variables on fish assemblage structure at the basin scale and within each river segment. First, we created three matrices based on the explanatory variables which included a site by local environmental variables matrix, a time matrix (i.e., monthly), and a space matrix (i.e., latitude and longitude coordinates of each sampling site). Second, similarity matrices created using Euclidean distances among sampling events and sites in the time and space matrices, respectively, were used in principal coordinates of neighbor matrix (PCNM) analyses to produce orthogonal eigenvectors representing temporal and distance components (Borcard and Legendre 2002; Angeler et al. 2009). Finally, a Hellinger-transformed response community matrix was created, and a Redundancy Analysis (RDA) was performed to assess the variation in the response community matrix explained by local environmental variables. If the RDA was significant, a forward selection procedure was performed on the axes and environmental variables of the RDA and PCNMs and only the significant axes and environmental variables were retained. Finally, using the significant axes (ranging from axes 1-3) from the PCNM and

RDA, the final variance partitioning was performed using the "varpart" function in the vegan package (Oksanen et al. 2022) and the significance of each factor's contribution was assessed using ANOVA-like permutation tests (Legendre and Legendre 2012).

We used a redundancy analysis (RDA) to examine relationships between fish assemblage composition and local environmental variables. We performed one model at the basin scale (i.e., with all 22 sites included) and three other models, one for each river segment individually (SF = 5 sites, DMF = 8 sites, and BRM = 9 sites) and included data from all sampling months. To assess potential multicollinearity among predictor variables, a Variance Inflation Factor (VIF) test was performed using the car package and a VIF threshold of 5 was used to determine if variables had issues of multicollinearity. Results of the VIF test showed that all variables in this study were below the threshold, suggesting no collinearity among predictor variables; thus, all variables were included in the analysis. Significance of the RDA models, axes, and individual

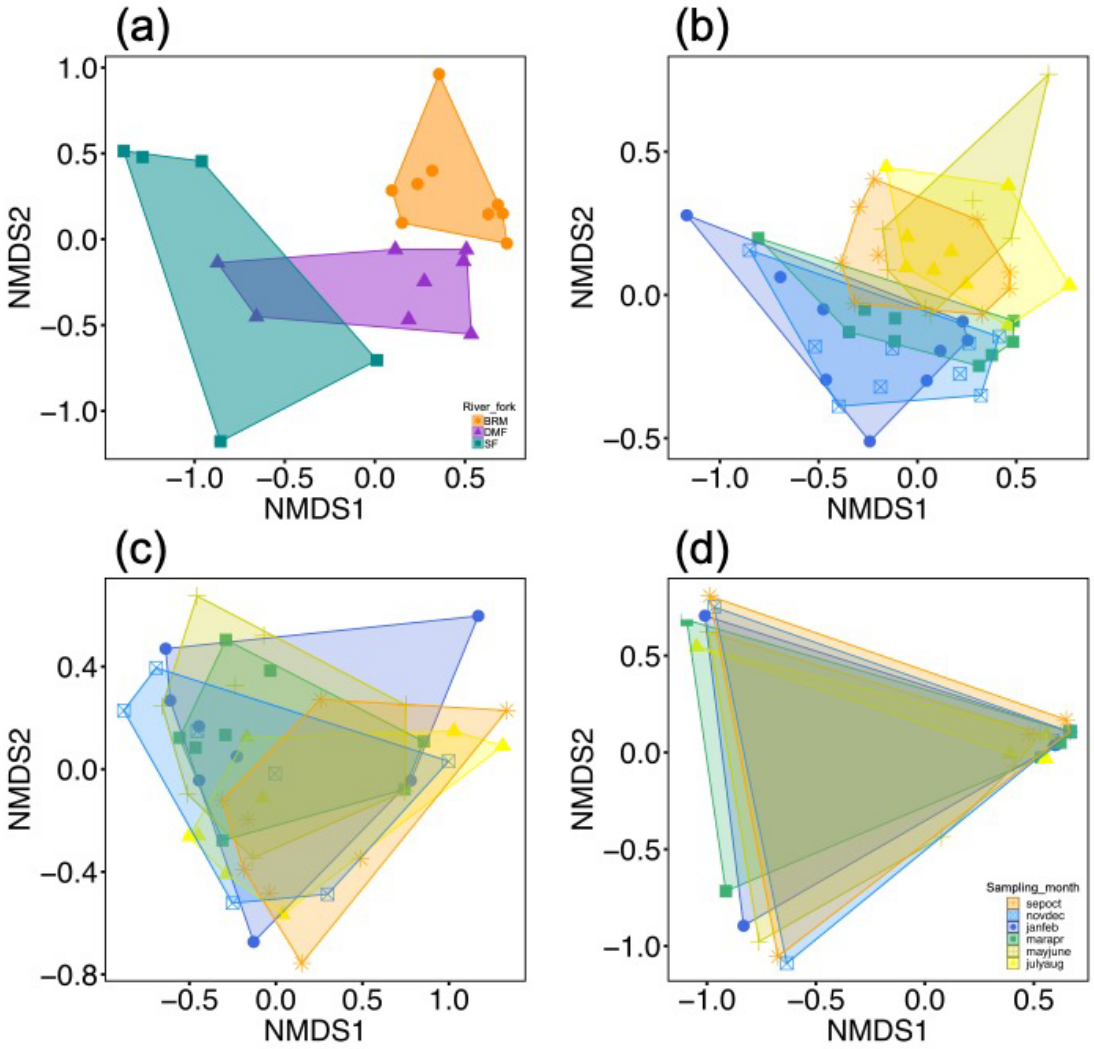


Figure 3: Non-metric multidimensional scaling (NMDS) of (a) fish assemblages based on summed abundances at three river segments and temporal NMDS of bimonthly fish assemblages at river segments (b) BRM, (c) DMF, and (d) SF.

variables were tested using ANOVA (999 permutations). The RDAs were performed and adjusted R2 values were calculated using the "RsquareAdj" function from the vegan package (Oksanen et al. 2022).

At the basin scale, the contributions of environment and space were significant ($p < 0.05$; Figure 4). The local environment accounted for 25% of the explained variance, and the forward selection process retained nine local environmental variables consisting of canopy coverage, wetted width, water conductivity, water temperature, stream flow, stream depth, macrophytes, undercut, and woody debris. Space (i.e., distance between sites) accounted for 4% of the variance, while the interaction between the environment and space accounted for 21%. Time did not show a significant contribution ($p = 0.19$) and did not account for any of the variance. At the

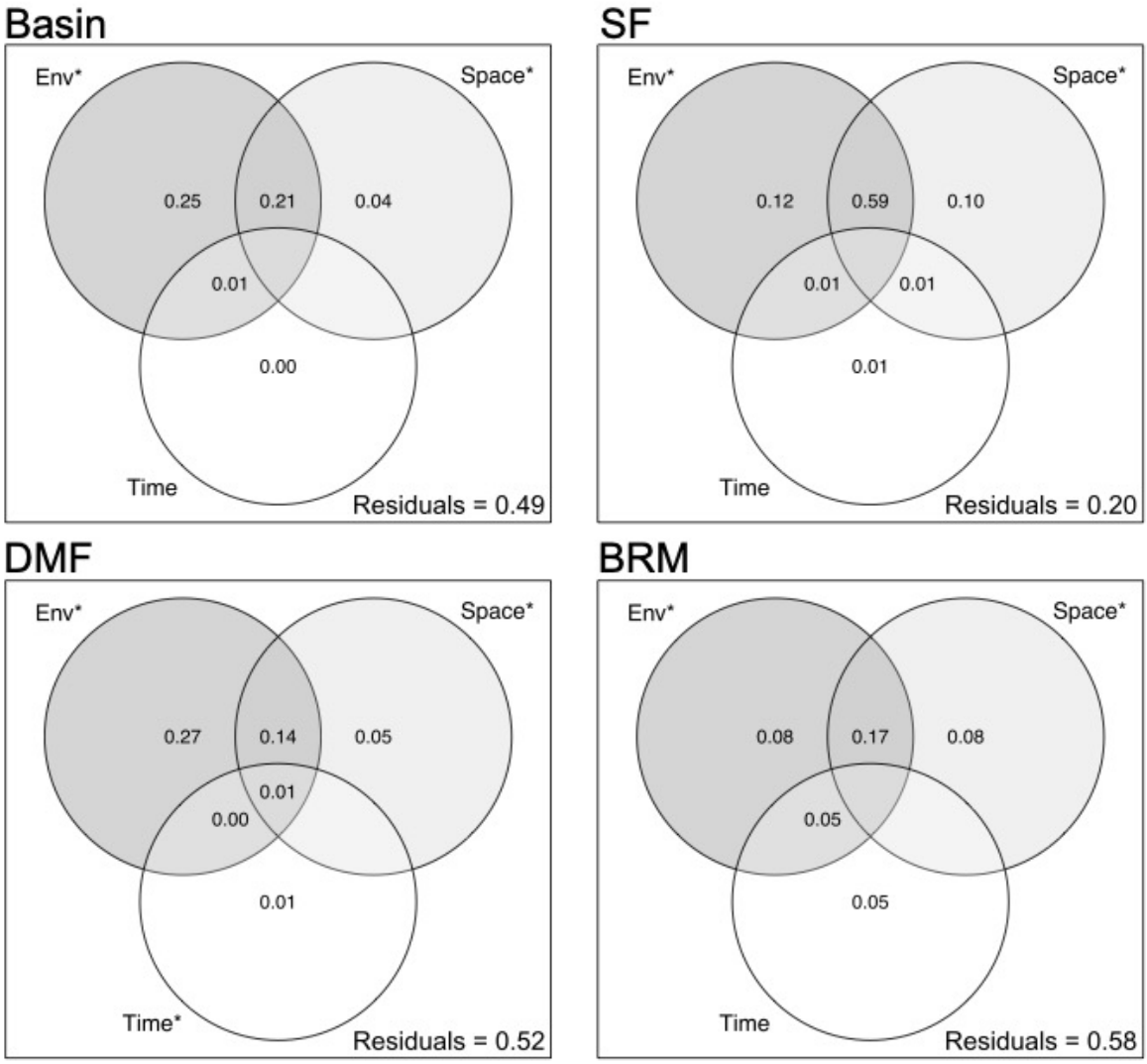


Figure 4: Venn diagrams summarizing the variance partitioning among local environmental variables (RDA axes), space (PCNM axes) and time (PCNM axes). Data were analyzed combining all observation samples from the entire basin, SF only, DMF only, and BRM only. Statistical significance was accessed for the unique contribution of local environment, space and time.

segment scales, in the SF segment, the contributions of environment and space were significant ($p < 0.05$; Figure 4), while time did not have a significant contribution ($p = 0.25$). Local environmental variables accounted for 12% of the variance, and the forward selection process retained seven variables including water conductivity, canopy coverage, stream flow, macrophytes, wetted width, depth, and pH. Space accounted for 10% and the interaction between the environment and space accounted for 59%. In the DMF segment, the contributions of all three factors were significant: environment ($p < 0.05$), space ($p < 0.05$), and time ($p = 0.02$) (Figure 4). Forward selection retained six variables including water conductivity, canopy coverage, wetted width, water temperature, bank undercut, and turbidity. These local environmental variables accounted for 27% of the variance while space accounted for 5%. The interaction between the environment and space accounted for 14% and while significant, time only accounted for 1% of the explained variance. Finally, in the BRM segment, the contributions of environment and space were significant ($p < 0.05$, Figure 4), with no contribution of time. Forward selection retained six variables: depth, water temperature, canopy coverage, Tamarix, woody debris, and stream flow, which accounted for 8% of the total variance. Space accounted for another 8% of the explained variance, and the interaction between the local environmental variables and space accounted for 17%, while time and environment explained 5%.

At the basin scale, RDAs 1 and 2 explained 41.34% of variation of fish species in relation to environmental variables (Figure 5a). RDA 1 separated river sites along a gradient based on their water chemistry and hydrologic features. Positive values along RDA 1 were associated with sites having high conductivity, high temperature, and greater coverage of macrophytes; fish species such as Red River Pupfish and Plains Killifish were related to these variables. Negative values on RDA 1 were explained by sites with deeper water and higher canopy coverage, and species such as Sharpnose Shiner, Smalleye Shiner, and Plains Minnow were associated with this axis. The RDA 2 separated sites based on stream flow and wetted width. Positive values corresponded with sites having narrow channels, faster flows, and the presence of Red Shiner (Cyprinella lutrensis), while sites with wide channels and low flows were negatively associated with this axis. At the segment scales, the RDA performed for the SF segment (RDAs 1 and 2) explained 69.57% of the total variation (Figure 5b). RDA1 explained a gradient based on stream morphology and conductivity, with positive values associated with wide channels, high flow, high conductivity, and the presence of Red River Pupfish, while negative values were associated with deep water, high canopy coverage, and the presence of Red Shiner. RDA2 separated sites based on pH, with high pH and the presence of the Plains Killifish positively associated with this axis. The RDA for the DMF segment (RDAs 1 and 2: 39.18% of the total variation, Figure 5c) separated fish assemblages along a gradient of water quality, canopy coverage, and the morphology of the sites. RDA1 separated sites based on water quality and canopy coverage, with positive values associated with high conductivity and the presence salt tolerant fishes (e.g., Red River Pupfish and Plains Killifish), while negative values grouped sites with turbid waters, high canopy coverage, and the presence of imperiled shiner species (e.g., Smalleye Shiner, Sharpnose Shiner, Plains Minnow, and Shoal Chub). Both temperature and stream morphology explained RDA 2. Wider channels were positively associated with this axis, while high temperatures were negatively associated with this axis, along with the presence of the Red Shiner. Finally, the RDA (axis 1 and 2) performed on the BRM segment yielded 31.62% of the total variation (Figure 5c), RDA1 separated stream sites based on depth and bank undercut. Sites with deep water and high bank undercut showed a positive association with the presence of Sharpnose Shiner, while Plains Minnow and Smalleye Shiner were negatively associated with these conditions. Along RDA2,

sites and associated fish were grouped based on temperature, flow, and canopy coverage. Positive values were associated with sites with high canopy coverage and the presence of Shoal Chub, while negative values were associated with sites having high water temperature and faster flow, with associated species being the Western Mosquitofish (Gambusia affinis) and Red Shiner.

Taken together, these assemblage-level results indicate that longitudinal variability in river hydrology and water chemistry are important local stream filters, sorting fish species in the upper Brazos River basin. In upstream river segments (SF and DMF), fish species were filtered from the regional species pool by local variables such as high salinity, low dissolved oxygen, and

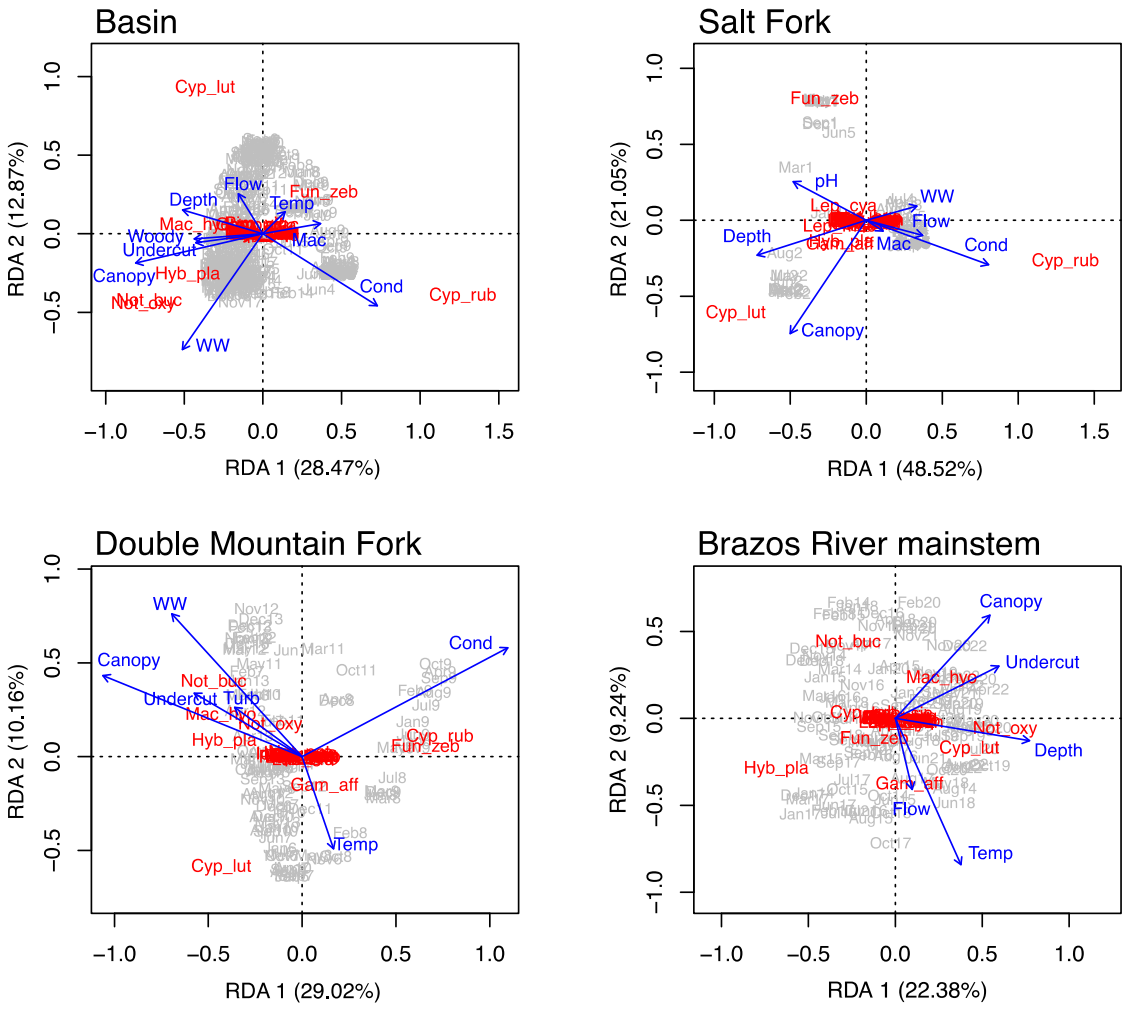


Figure 5: Redundancy Analysis (RDA) based on Hellinger transformed species abundance and local environmental variables at the basin scale and Salt Fork, Double Mountain Fork, and Brazos River mainstem river segments. All presented model axes are statistically significant ($p < 0.05$). Basin ($F_{5,96} = 9.49$, $R2 = 0.46$); SF ($F_{7,47} = 17.39$, $R2 = 0.68$); DMF ($F_{6,80} = 10.35$, $R2 = .39$); BRM ($F_{5,96} = 9.49$, $R2 = 0.30$). Gray text represents the sampling events with the month sampled followed by the site number.

high temperatures, whereas fish species that can tolerate these physiological stressors were present year-round. In downstream segments (BRM), lower salinity, continuous flow throughout the year, and greater environmental stability corresponded with greater species diversity.

Using the full two-year dataset of monthly seine and environmental data, we further explored population responses of individual taxa to environmental gradients. Identification of environmental conditions associated with threshold responses (i.e. non-linear population response along an environmental gradient) contributes to understanding ecological mechanisms structuring communities and has become increasingly helpful for informing and developing effective management strategies (Dodds et al. 2010; Groffman et al. 2006). Threshold indicator taxa analysis (TITAN2) was used to identify individual species threshold responses to changes along environmental gradients representing instream habitat quality (Baker and King 2010). TITAN2 uses indicator species scores (IndVals) to analyze and identify changepoints based on the occurrence and abundance of taxa, then identify directionality (increase or decrease) of individual taxa responses along an environmental gradient. Permutations (1000) provide estimated significance of IndVals by comparing observed scores to observations that are randomly ordered along the environmental gradient. Analyses indicate whether species exhibit increasing or decreasing abundance along an environmental gradient, whether that pattern of change is representative of a threshold response, and the optimum changepoint for each response. Bootstrapping (1000 repetitions) provided two diagnostic indices to evaluate the quality of the group assignments: purity and reliability. Reliability is the estimated proportion of changepoints that consistently result in grouping of taxa – only taxa with high reliability ($\geq$0.95) are considered indicator taxa. Purity is the proportion of response direction (z- or z+) passing changepoints that agree with the observed response – only taxa with purity $\geq$0.95 were used. The first axis (PC1; Figure 6) from principal components analysis of the full suite of environmental data was included as a composite gradient, and significant individual environmental gradients used for threshold analyses were flow (m/s), wetted width (m), and depth (m).

Sharpnose and Smalleye shiners exhibited strong positive threshold responses to PC1 (Figure 7), and individual gradients of flow (Figure 8), wetted width (Figure 9) and depth (Figure 10). Specifically, those responses indicate that large increases in abundances of these taxa are associated with thresholds of flow > 0.075 m/s, wetted width > 10 m, and depth > 0.2 m (approximate values from combining thresholds for both species). Results for the composite gradient (PC1; Figure 7) complement the individual gradient results. Notably, Shoal Chub (*Macrhybopsis hyostoma*), which is listed as a Species of Greatest Conservation Need (SGCN) in Texas, exhibited similar results to those observed for Sharpnose and Smalleye shiners. In contrast, Red River Pupfish (*Cyprinodon rubrofluviatilis*), which is listed as threatened in Texas, and Plains Killifish (*Fundulus zebrinus*) exhibited negative threshold responses to those same gradients. These results complement the aforementioned community structure analyses.

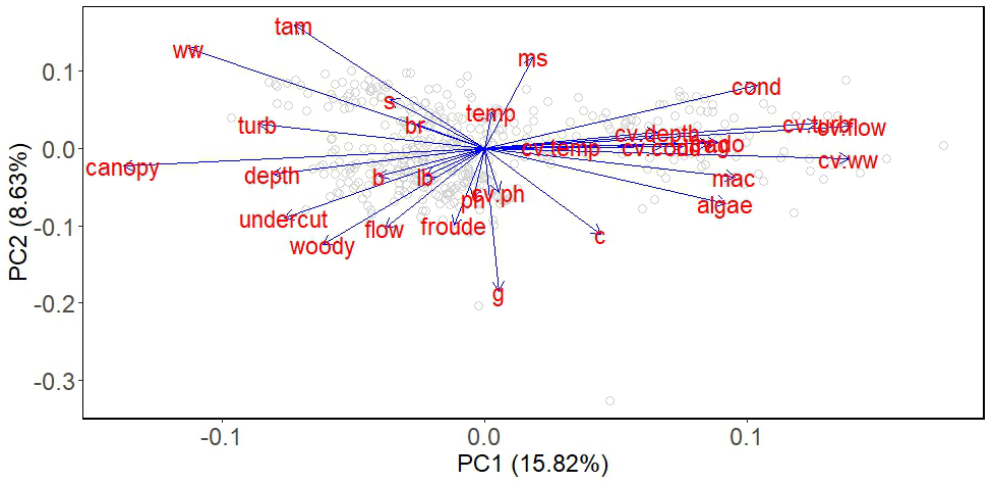


Figure 6: Principal components analysis of environmental variables quantified at each site during two years of monthly surveys. Variables quantified at multiple points along transects (e.g. flow, depth) are represented by mean and CV for each site/event for such variables.

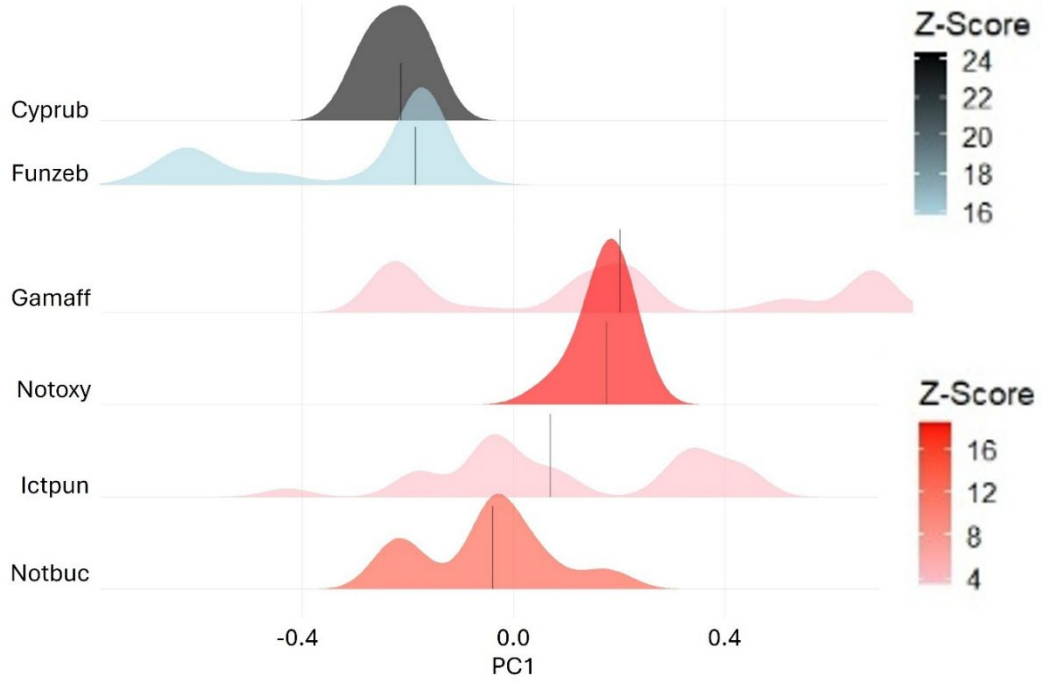


Figure 7: Taxon-specific responses of pure and reliable indicator species to PC1 composite gradient. Positive values along the composite gradient are associated with increases in depth, canopy coverage, turbidity, and wetted width. Negative values are associated with increases in coefficients of variation for hydrologic variables (cv.flow, cv.ww, cv.depth, cv.cond) and instream descriptive variables such as percent macrophyte and algae coverage. Taxa that respond positively to the gradient are shown in red, negative responding taxa are shown in blue. The darker the color, the greater the magnitude of species abundance and change occurring along the gradient. Vertical black lines represent the median changepoints for taxa across all replicates. Height and shape of the curve represent densities of bootstrapped responses along the gradient.

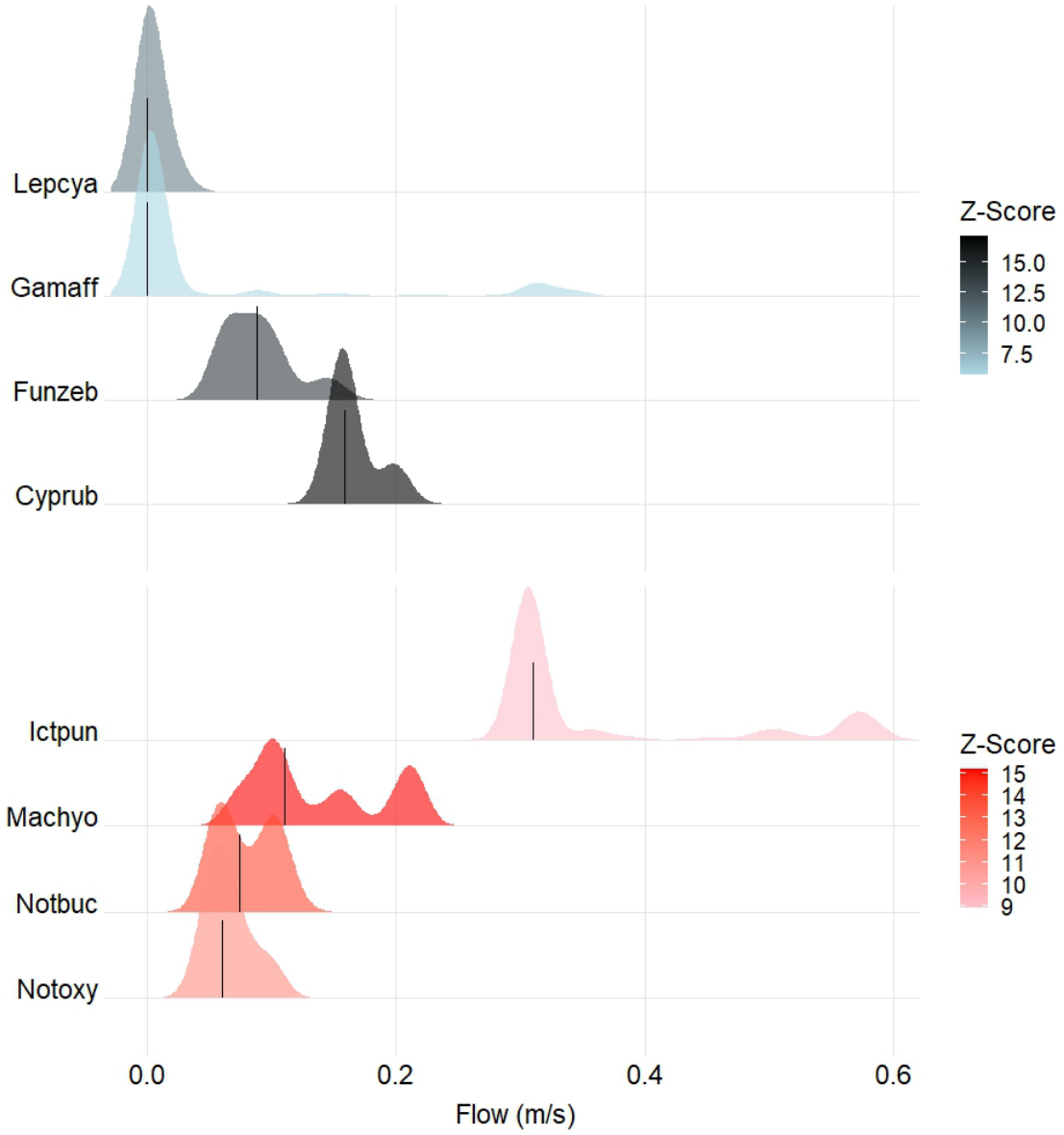


Figure 8: Taxon-specific responses of pure and reliable indicator species to flow (m/s). Taxa that respond positively to the gradient are shown in red, negative responding taxa are shown in blue. The darker the color, the greater the magnitude of species abundance and change occurring along the gradient. Vertical black lines represent the median changepoints for taxa across all replicates. Height and shape of the curve represent densities of bootstrapped responses along the gradient.

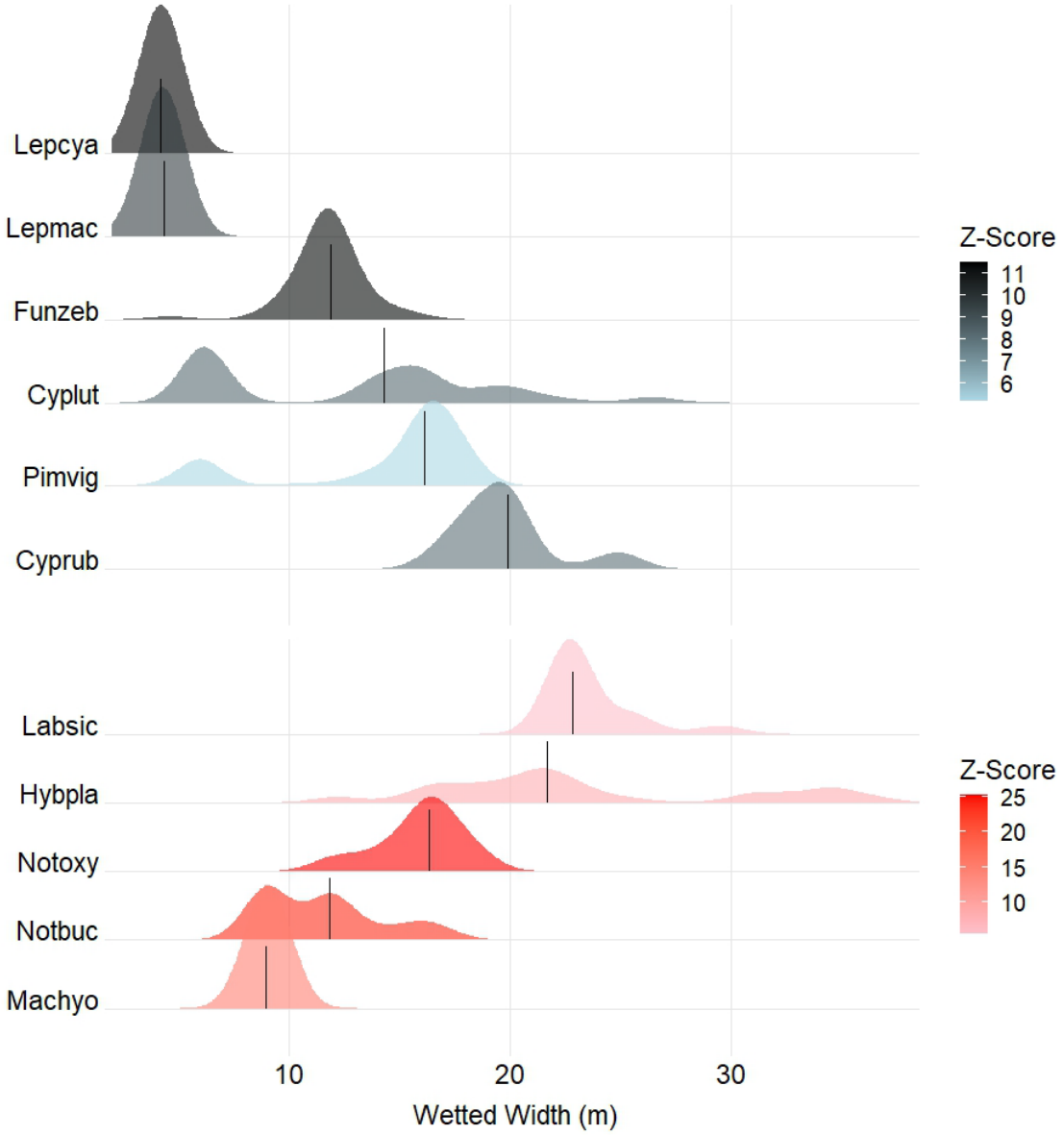


Figure 9: Taxon-specific responses of pure and reliable indicator species to wetted width (m). Taxa that respond positively to the gradient are shown in red, negative responding taxa are shown in blue. The darker the color, the greater the magnitude of species abundance and change occurring along the gradient. Vertical black lines represent the median changepoints for taxa across all replicates. Height and shape of the curve represent densities of bootstrapped responses along the gradient.

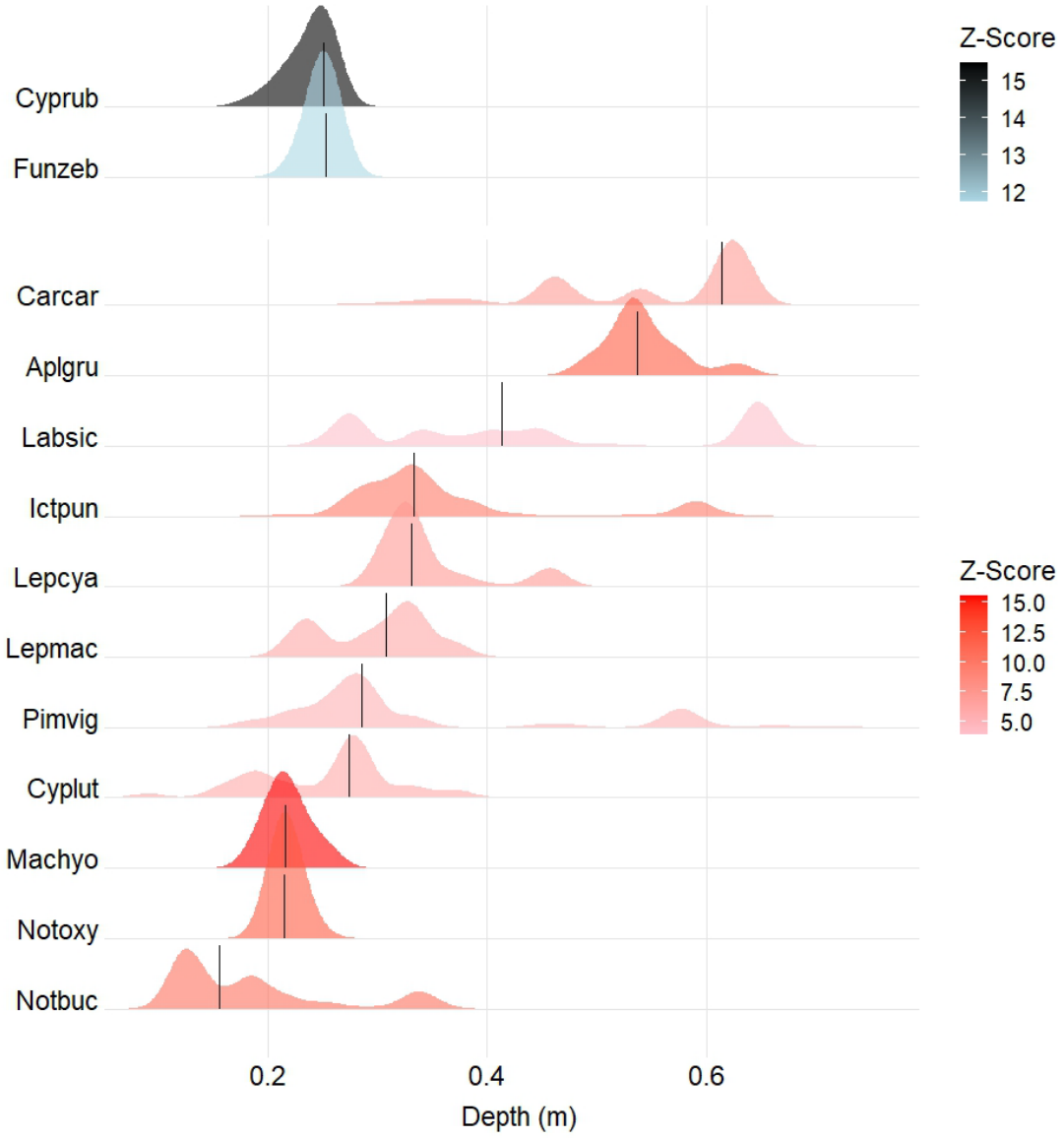


Figure 10: Taxon-specific responses of pure and reliable indicator species to depth (m). Taxa that respond positively to the gradient are shown in red, negative responding taxa are shown in blue. The darker the color, the greater the magnitude of species abundance and change occurring along the gradient. Vertical black lines represent the median changepoints for taxa across all replicates. Height and shape of the curve represent densities of bootstrapped responses along the gradient.

Specific threshold values for significant environmental gradients (i.e. flow, wetted width and depth) can be integrated to identify conditions representing highly suitable habitat, assuming that relative abundance correlates with habitat suitability. Analysis of site conditions relative to threshold values for flow, wetted width and depth for each species indicate that >85% and >82% of individuals of Sharpnose and Smalleye shiners, respectively, were collected when all three variables exceeded threshold values (Figure 11). Conditions that meet all three thresholds

represent highly suitable habitat, which we refer to as 'Goldilocks' conditions because only minor reductions below thresholds from those conditions represent significant reduction in habitat suitability, as evidenced by relative abundances. For example, environmental conditions exceeding only a single threshold (flow, wetted width or depth) account for <1% of abundance for each species, and two of three thresholds met (flow/width, flow/depth, width/depth) account for 2-7% and 2-11% for Sharpnose and Smalleye abundances, respectively (Figure 11).

The frequency of availability of habitat conditions for each category varied among the Brazos River mainstem, Double Mountain Fork and Salt Fork and over time. For both species, high quality habitat (based on the criteria that all three thresholds were met) was consistently observed in the Brazos River mainstem (Figures 12 and 13). Lesser suitable habitat (i.e. two of three thresholds met) was commonly observed in the Double Mountain Fork for Sharpnose Shiners (Figure 12). Similarly, lesser suitable habitat (i.e. two of three thresholds met) was commonly observed in the Double Mountain Fork for Smalleye Shiners and all three thresholds were exceeded in at least one site during most sampling events (Figure 13). The occurrence of high-quality habitat in the Salt Fork was rare and episodic for both species and especially for Sharpnose Shiner (Figures 12 and 13). The aforementioned patterns reflect the spatial distribution of abundances and proportional abundances (relative to the total of all fish species) for Sharpnose and Smalleye shiners (Figures 14 and 15), but provide a unique contribution by identifying the suite of parameters that together correspond with strong threshold population responses and the relative availability of those conditions in space and time.

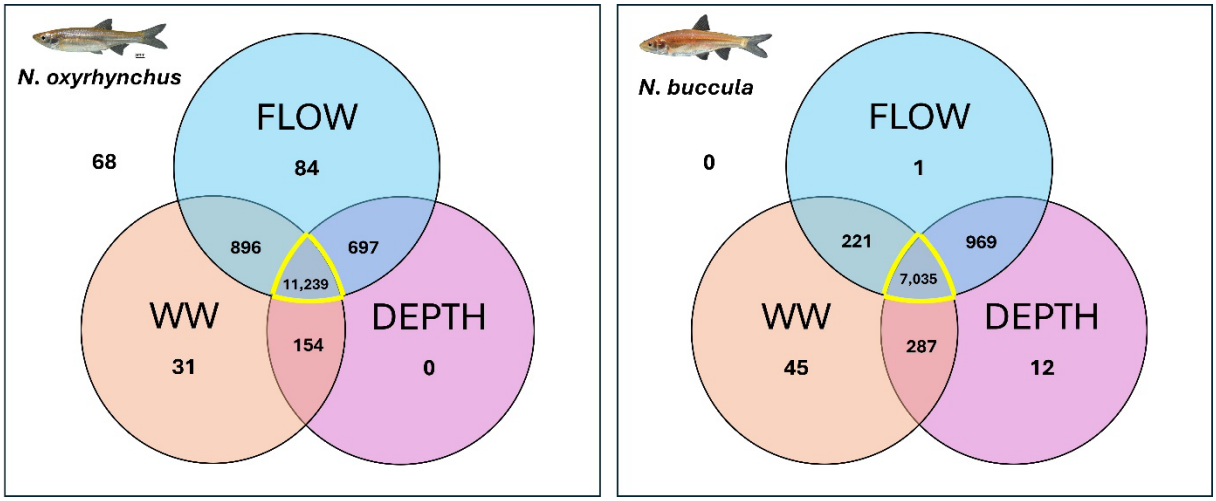


Figure 11: Venn diagrams indicating the relative abundances of Sharpnose and Smalleye shiners collected under different conditions during 24 monthly sampling events at 22 sites in the Upper Brazos River basin. Numbers within circles for flow, wetted width and depth indicate the number of individuals collected at sites when threshold conditions for those variables were met. Options represent each individual gradient alone (i.e. values for the other two gradients did not exceed threshold values), events when two of the three gradients exceeded threshold values (overlap of two circles only) and events when all threshold conditions were exceeded for all three gradients (center of plot with yellow border). The number of individuals collected when no thresholds were exceeded is within the white space outside of the circles.



Figure 12: Frequency of habitat conditions relative to thresholds of flow, wetted width and depth for Sharpnose shiner, during monthly surveys over two years for the three sub-basins of the Upper Brazos. Frequencies represent the proportion of sites within the sub-basin during a monthly sampling event that fall within each of 8 possible categories depicted in Figure 11. 'Goldilocks' conditions, i.e. all three thresholds met, are yellow and account for >85% of total abundances. Conditions where 2/3 thresholds met are in different shades of green and together account for approximately 13% of total abundance.

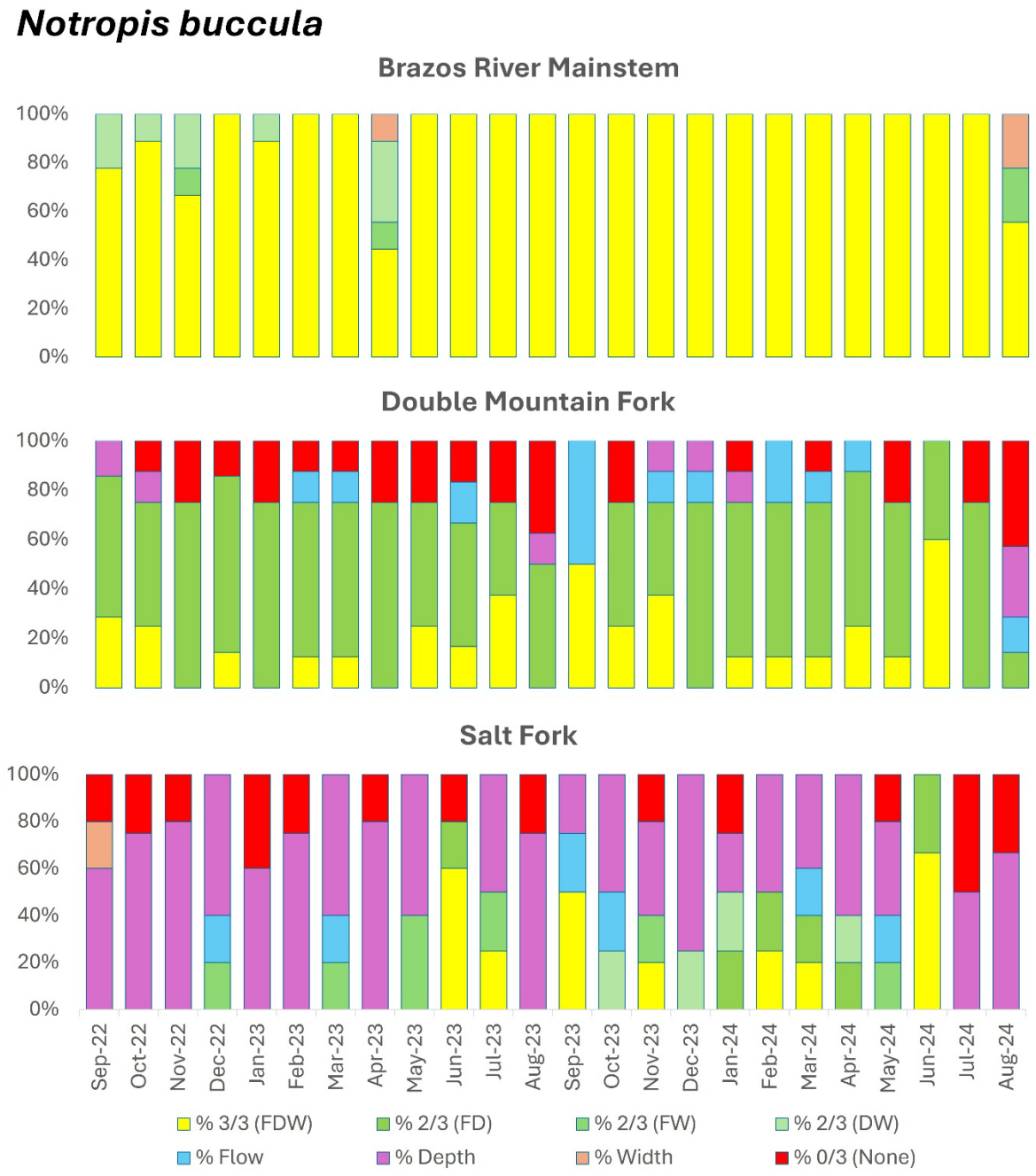


Figure 13: Frequency of habitat conditions relative to thresholds of flow, wetted width and depth for Smalleye shiner, during monthly surveys over two years for the three sub-basins of the Upper Brazos. Frequencies represent the proportion of sites within the sub-basin during a monthly sampling event that fall within each of 8 possible categories depicted in Figure 11. 'Goldilocks' conditions, i.e. all three thresholds met, are yellow and account for >82% of total abundances. Conditions where 2/3 thresholds met are in different shades of green and together account for approximately 17% of total abundance.

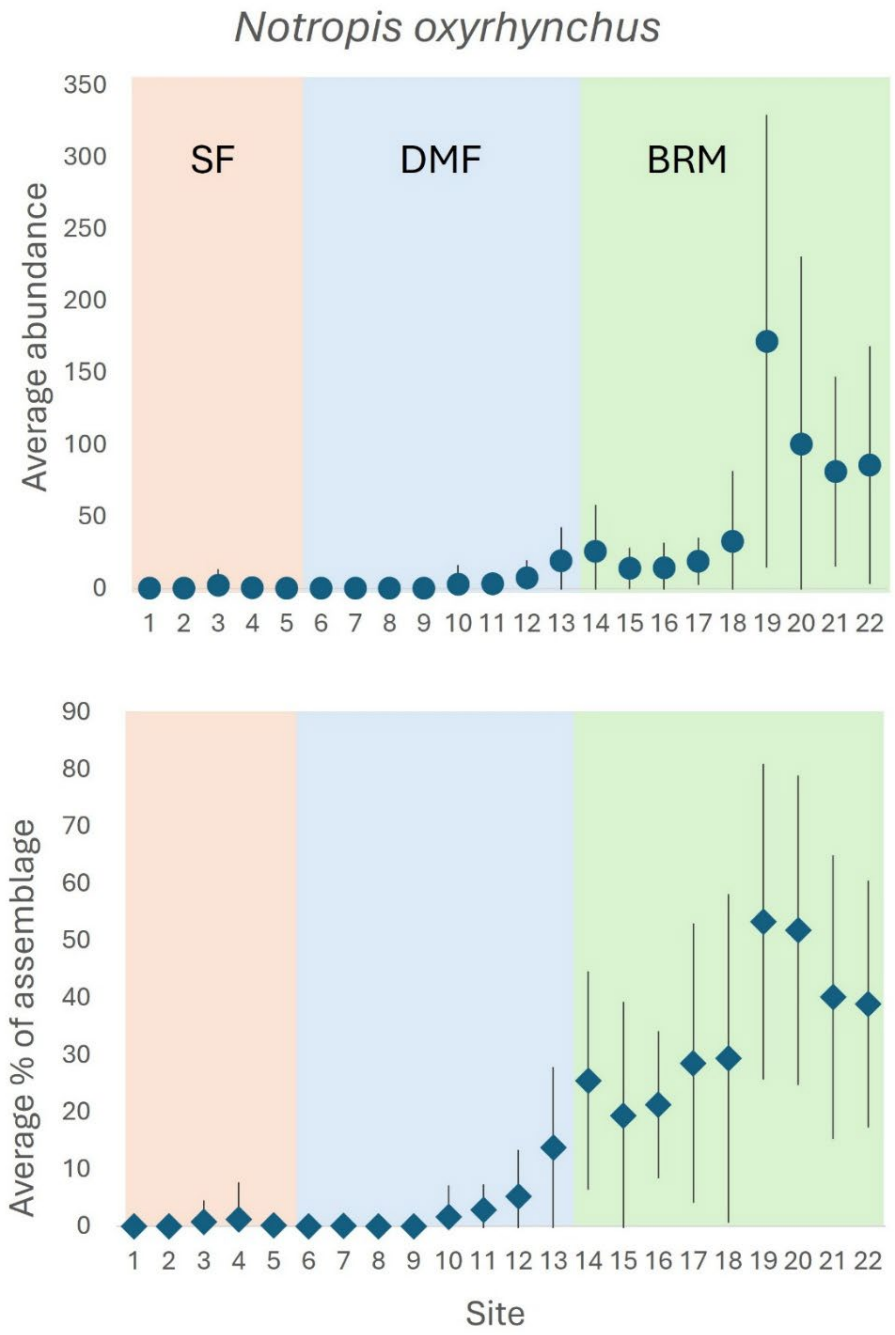


Figure 14: Average abundance (± 1SD) and average percent of total fish abundance (± 1SD) of Sharpnose Shiner at all 22 sampling sites in the Upper Brazos River basin. Shading distinguishes sites in the Salt Fork (SF), Double Mountain Fork (DMF) and Brazos River mainstem (BRM). See Figure 1 for spatial arrangement of sites and Figure 12 for frequency of attaining highly suitable habitat in each sub-basin.

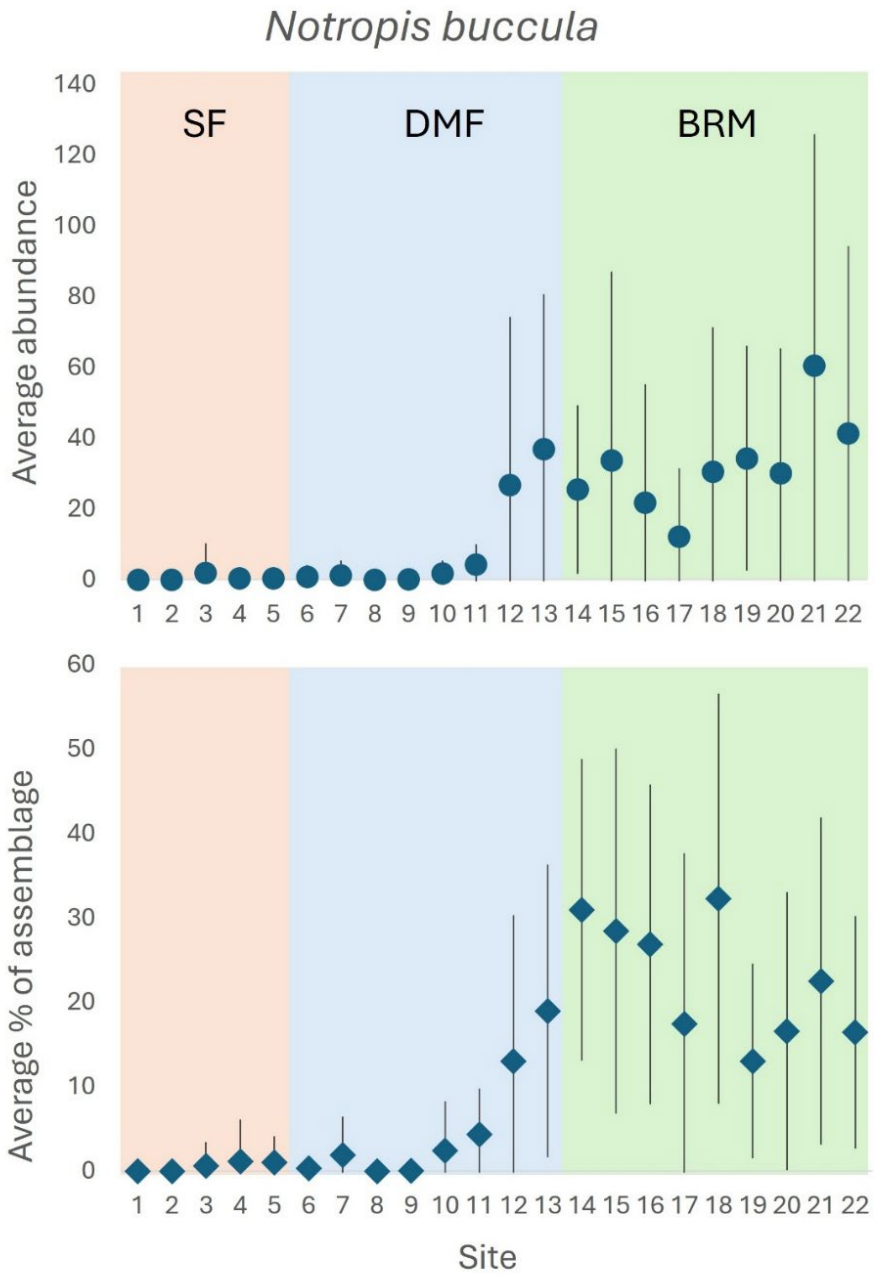


Figure 15: Average abundance (± 1SD) and average percent of total fish abundance (± 1SD) of Smalleye Shiner at all 22 sampling sites in the Upper Brazos River basin. Shading distinguishes sites in the Salt Fork (SF), Double Mountain Fork (DMF) and Brazos River mainstem (BRM). See Figure 1 for spatial arrangement of sites and Figure 13 for frequency of attaining highly suitable habitat in each sub-basin.

In an attempt to understand how individual movement affects the patterns of distribution reported above, especially for local populations recolonizing following drought or as individuals prepare for spawning, a subset of age-2 individuals of Sharpnose (N=488) and Smalleye (N=494) shiners from multiple sites (N=9) were tagged with passive integrated transponder (PIT) tags between February 28 and July 28, 2025 (Figure 16). Based on previously reported size distribution data for Sharpnose and Smalleye shiners, results from previous studies and conversations with technicians at Biomark, age-2 individuals (>45 mm TL) of both species were expected to be of suitable size to be tagged with 9mm Biomark HPT PIT tags in the body cavity. Individuals were collected via targeted seining for Sharpnose and Smalleye shiners of the appropriate size on dedicated field campaigns, i.e. not part of regular sampling described above, to minimize handling stress. Tagging was conducted by making a small incision with the tip of the syringe on the tag injector and gently injecting the tag into the body cavity (i.e. the tag is pushed in from the tip of the syringe but the syringe does not deeply penetrate the body cavity). Previous studies using this technique and similarly sized PIT tags in shiners and similarly sized fishes found high tag retention (>95%), high survivorship (>85%, often not significantly different from control treatments), no significant impact of tagging on growth for individuals of the target size (>45 mm TL) and no disruption of spawning (Bolland et al. 2009, Bangs et al. 2013, Cary et al. 2017, Pennock 2017, Allan et al. 2018, Tiffan et al. 2019, Pennock and Bruckerhoff 2020, Schumann et al. 2020, Schumann et al. 2021). We endeavored to further improve survivorship (i.e. reduce general handling mortality) through our field protocol of holding fish in cool aerated stream water pending tagging, dosing with MS-222 to sedate individuals before tagging to reduce handling stress and potential for injury, and holding fish in an aerated recovery tank while recovering from tagging and sedation to aid in acclimation for return to the stream and for treatment with Stress Coat or other water conditioners that improve the slime coat (which could be damaged by handling), facilitate healing and reduce susceptibility to disease and infection.

Tagged individuals were held in aerated recovery tanks (max holding time 364 minutes, median 68 minutes) and water quality was monitored throughout. Observed acute mortality, i.e. individual was dead or could not swim out of the bucket on its own when placed into the stream at the end of the holding time, was 3.56% (35 of 982 individuals). Mixed effects logistic multiple regression was used to test for factors associated with mortality while controlling for effects of sample site and sampling campaign. Fixed effects were length, water temperature and pH, and random effects were site and site/date (i.e. site sampling campaign). From the possible models, only Motality ~ Length + (1|Site) was interpreted because inclusion of other parameters resulted in singularity. Length was a significant predictor of acute mortality ($P<0.001$), with an estimate of -0.284 and odds ratio of 0.753, indicating that with every unit increase in TL, mortality reduces by approximately 25%.

Surveys to detect tagged fish were conducted by two technicians wading through the site in a zig-zag pattern from downstream to upstream with each technician starting on opposite sides of the stream and crossing back and forth, with one just ahead of the other. This approach was meant to help ‘herd’ fish to move into the path of a technician. Detections were conducted using Biomark handheld antennae (similar in appearance to metal detectors) as well as a larger floating antenna that has a larger read range (up to 40” for the proposed 9 mm tag) while enabling the technician to be farther away and not disrupt the fishes being monitored. Dozens of surveying events were conducted under various field conditions, initially focusing on sites where individuals were originally tagged due to the expectation that most individuals do not move from

the site capture over the time scales in consideration. Only 18 tag detections of seven unique tags were recorded between July 15 and October 5, 2025 (between 79 and 205 days after tag was deployed). On later survey dates, seining was also conducted in an attempt to capture a tagged fish to validate presence and that the tag had been retained and the individual was alive. Even though we caught many individuals of the appropriate size during those surveys, we never caught a tagged individual. At this point, we are unable to verify if tagged individuals survived or if the few detections were of tags in the sediment either ejected from the fish or from a mortality event and the tag remained. It is also worth noting that we tagged a relatively small number of individuals, late in their life-cycle, and from a large open river system. Given that, detections of tagged fish could be considered unlikely. Further experimental work is necessary to validate longer-term survival and whether tagging affects other aspects of fish biology and ecology.

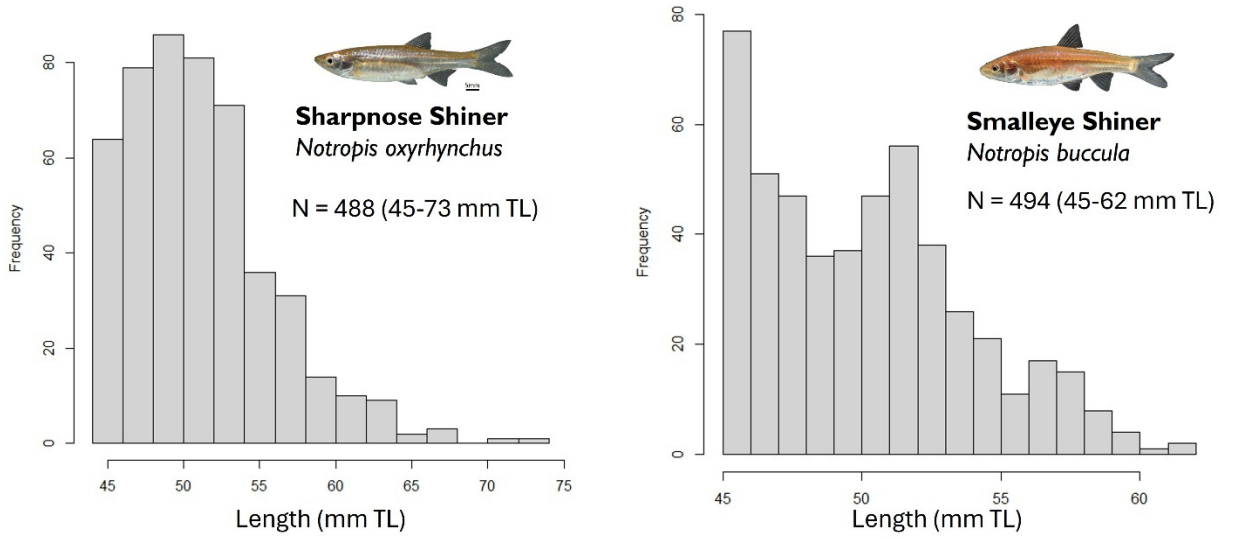


Figure 16: Size-frequency distributions for individuals of Sharpnose and Smalleye shiners tagged with PIT tags. Total sample sizes are for individuals tagged at all sites and events aggregated.

Water samples collected for eDNA analyses were thawed prior to filtration and stored at 4 °C on the day of filtration. All samples were filtered in a Class II Type A2 Biosafety Cabinet (BSC) cleaned with 100% ethanol and UV-sterilized for 15 minutes. All filtration supplies were cleaned following the same established cleaning protocols as the collection bottles (Goldberg et al., 2016). Samples were filtered using JoanLab VP-10L diaphragmatic pumps connected to side-arm vacuum flasks with sterilized, reusable Sterlitech filter housings and 47mm diameter, 0.45 µm pore size nitrocellulose mixed ester (MCE) Sterlitech filters. When filters became clogged (e.g., at high-turbidity sites), multiple filters were used to collect the entire 500 mL water sample. Each filter was halved using sterilized plastic scissors and carefully rolled into RNase/DNase-free 2 mL screw-cap tubes with sterilized forceps. When multiple filters were used, we halved each filter and took equal proportions of each halved filter to equal the area of one half of a filter. For all samples, filters were storaged in tubes at −80 °C until extraction. The unused halves of filters were stored at −80 °C for archival.

Extractions were carried out in sterilized Class II Type A2 BSCs located in a separate area of the lab dedicated to extractions and PCR preparation. All lab surfaces in the extraction

area that could not be UV sterilized were cleaned before and after DNA extractions using 50% commercial bleach (6% hypochlorite). All non-chemical materials within the extraction cabinet were UV sterilized prior to extraction and only filtered pipette tips were used to prevent potential contamination from pipettes.

DNA was extracted from half of each filter using the Qiagen DNeasy Blood & Tissue Kit (Qiagen, Hilden, Germany) with a modified protocol optimized for environmental water samples. When multiple filters were involved, each filter was cut into sections to ensure each piece was equal in volume to half a filter (as above). The remaining half of each filter was stored at −80°C for archival purposes in case of failed extractions. The filter halves to be extracted were placed in RNase- and DNase-free 2 mL screw-cap tubes. To each tube, 360 µL of Buffer ATL (Qiagen, Hilden, Germany) and 40 µL of Proteinase K were added, then vortexed for 30 seconds to thoroughly submerge and coat all sections of the filter with the lysis mixture. Samples were then incubated at 56°C and shaken at 10 RPM in a Benchmark Roto-Therm™ Incubated Rotator for 48 hours to maximize DNA extraction (Carim et al., 2016).

Upon removal from the hybridization oven, 400 µL of Buffer AL and 400 µL of molecular-grade EtOH were added to each sample. Samples were then vortexed for 15 seconds and incubated at 70 °C for 10 minutes. After the second incubation, samples were vortexed for another 5 seconds and spun down before adding 600 µL to the Qiagen Mini Spin column (Qiagen, Hilden, Germany). Spin columns were centrifuged at 20000 x g for 2 minutes. The Mini Spin collection tube was discarded and replaced before the remaining supernatant was added to the sample and centrifuged again. The Qiagen DNeasy Blood & Tissue protocol was followed for the rest of the procedure. Eluted DNA extracts were stored at 4°C to minimize freeze-thaw cycles until PCR and then moved to −80 °C for long-term storage.

A novel 16S vertebrate primer, "RiVer" [F: AGACGAGAAGACCCTWTG, R: GGATTGCGCTGTTATCCC], was created from the existing 16S marine vertebrate primer MarVer3 (Valsecchi et al., 2020) because existing 12S and 16S fish primers that are commonly used for similar applications were found (in silico and pilot studies) to target regions that lacked resolution for much of the Upper Brazos fish assemblage. Primer redesign was necessary because preliminary evaluation of commonly used fish metabarcoding primer sets indicated that several Upper Brazos taxa, including the focal shiner species, either shared identical or nearly identical amplicon sequences at commonly targeted loci or showed primer-binding mismatches that reduced amplification efficiency in preliminary trials. The purpose for developing the RiVer primer set was, therefore, to 1) improve amplification consistency across the Upper Brazos fish assemblage and 2) target a 16S region with sufficient sequence variation to distinguish the focal species from closely related co-occurring taxa whenever possible.

RiVer was tested in silico against Texas and Upper Brazos fish species to assess primer affinity and resolution for each species. The in silico assessment included available mitochondrial 16S reference sequences for fish species known or expected to occur in the Upper Brazos River watershed, with particular emphasis on the focal Sharpnose and Smalleye shiners and closely related or morphologically similar cyprinid species. Primer affinity was evaluated by examining primer-binding mismatches, especially mismatches near the 3′ end of each primer, expected amplicon length, and predicted amplification success across target and non-target taxa. Taxonomic resolution was evaluated by comparing expected amplicon sequences among species and identifying cases where species shared identical, nearly identical, or diagnostically distinct sequences.

Optimal PCR conditions were determined in a pilot study testing various Brazos eDNA samples. The pilot study was designed to represent the range of field conditions encountered during the project—including samples collected during periods with a range of turbidity, conductivity, and stream temperatures—that could have led to PCR inhibition and impacted DNA amplification. PCR optimization compared annealing temperature profiles, dilution of template DNA, replicate consistency, and amplification strength across representative samples. Final PCR conditions were selected based on consistent amplification of environmental samples, successful amplification of positive controls, absence of amplification in non-template controls, and reduced evidence of inhibition following template dilution.

All PCR preparations were carried out inside sterilized biosafety cabinets located in a dedicated and isolated area of the lab for extractions and PCR preparation. No post-PCR products were allowed in this lab space. To reduce contamination risk, all pre-PCR work followed a unidirectional workflow from DNA extraction to PCR setup, with physically separated pre-PCR and post-PCR spaces. Work surfaces, pipettes, tube racks, and other materials were decontaminated before and after use using the same bleach-based cleaning, ethanol wipe-downs, and UV exposure described above. Filtered aerosol-resistant pipette tips were used for all DNA handling steps, and PCR setup was performed with dedicated pre-PCR pipettes and consumables.

eDNA samples were diluted tenfold with Tris-HCl pH 8.5 before PCR to limit degradation and reduce inhibition. A ten-fold dilution was selected because pilot testing indicated that undiluted extracts from some Brazos River samples were more likely to show reduced or inconsistent amplification, consistent with environmental PCR inhibition. Dilution was therefore used as a standardized inhibition-mitigation step across samples while still retaining sufficient template DNA for detection. Template DNA was amplified using the RiVer 16S vertebrate primer. Three replicate PCRs were performed in 25 µL reactions [12.5 µL Promega GoTaq Hot Start Master Mix, 0.5 µM primers, 5 µL template], and combined prior to the first DNA cleanup. Amplification followed a step-up protocol (8/11/11/10 cycles at 54/55/56/57°C, respectively), modified from the original (Valsecchi et al., 2020) protocol.

Post-PCR products were handled in a separate lab from all pre-PCR processes. Combination, PCR cleanups, and index PCR occurred within sterilized biosafety cabinets. Lab spaces and materials were cleaned following the same protocols used in pre-PCR steps. To control for contamination, each PCR plate included two non-template controls in separate quadrants. Field and extraction blanks were also included on PCR plates alongside their respective samples to monitor contamination throughout the pipeline. A positive control was included on every plate as a secondary measure for contamination, index hopping, and to identify errors in bioinformatic filtering strategies. Controls were used as quality controls to make decisions during both laboratory processing and bioinformatic filtering. Non-template controls were used to detect PCR-plate contamination, while field and extraction blanks were used to identify contamination introduced during sample collection or DNA extraction. Positive controls were used to verify amplification and indexing success and to detect potential index misassignment. Any ESVs detected in blanks or controls were reviewed during downstream filtering, and detections were removed or flagged when their distribution suggested contamination, index hopping, or laboratory carryover rather than true environmental occurrence.

The three PCR replicates were pooled and purified using a 1.8x ratio of AMPure beads prior to indexing. Index PCR was performed using the Illumina® DNA/RNA UD Tagmentation

Indexes in 25 µL reactions [12.5 µL Promega GoTaq Hot Start Master Mix, 5 µL water, 5 µL tagmentation indexes, and 2.5 µL pooled and purified template]. The indexed libraries were cleaned with a 1.8x AMPure bead ratio. Prior to sequencing, cleaned, indexed libraries were assessed using an Agilent Technologies TapeStation, normalized to reduce among-sample variation in sequencing depth, and pooled for sequencing on an Illumina MiSeq v2 (2×250 bp) at the UNT Genomics Center. Sequencing success was evaluated using total reads per run, read quality, recovery of positive controls, absent target reads in negative controls, and retention of sufficient reads per environmental sample after quality filtering.

For scalability and reproducibility, the Global ESV Metaworks workflow was used for all bioinformatic processing (Porter & Hajibabaei, 2022). Bioinformatic processing followed a standardized ESV-based workflow rather than an operational taxonomic unit clustering approach, allowing exact sequence variants to be tracked consistently across sequencing runs and samples. Processing included demultiplexing, primer trimming, read merging, quality filtering, removal of low-quality or non-target reads, assignment of ESVs, and taxonomic classification. Species assignments were determined using a custom bioinformatic pipeline created for the fish assemblage in the Brazos River watershed. This pipeline capitalized on an RDP classifier (Wang et al., 2007) employed through Metaworks (Porter & Hajibabaei, 2022). Our (~230 bp) 16S metabarcoding amplicon provides strong resolution for the target taxa within the Upper Brazos River fish assemblage, but, like any metabarcoding amplicon, it cannot be assumed to distinguish all closely related fish species globally; consequently, taxonomic calling was implemented using a system-informed, evidence-weighted framework rather than unconditional global species assignment. In the first pass, fish ESVs (ESVs assigned to Actinopterygii by Metaworks) were provisionally assigned based on top hits in NCBIs Basic Local Alignment Search Tool (BLAST), with 100% query coverage. Ties were evaluated against the list of species and sampled by seine throughout the project. Ties containing exactly one sampled species were resolved to that species, ties containing multiple sampled species were retained as ambiguous, and ties lacking sampled species were conservatively reduced to genus-level calls (preferring genera represented in the system when overlap existed, because multiple genera in this system cannot be distinguished below the genus level, e.g., Macrhybopsis and Cyprinodon).

In the second pass, provisional calls were refined using percent-identity thresholds and a conservative MetaWorks 99%-accuracy fallback. Species calls not present in the sampled list were retained only when the maximum BLAST identity was high (≥98%). Otherwise, they were downgraded to the genus level. If the resulting genus was not present among sampled system genera and percent identity was <95%, the call was replaced with the most specific MetaWorks rank (genus, family, order, etc.) passing conservative bootstrap probability thresholds (genus ≥ 0.95; family ≥ 0.30). Ties with no sampled species were further evaluated such that low-identity (<95%) or multi-genus ties were reassigned to the MetaWorks fallback, whereas higher-identity ties preferentially resolved to a genus present in the sampled system when available. ESVs lacking any BLAST call were also assigned using the MetaWorks fallback. This approach limits overconfident global species calls when the locus is non-diagnostic, while still allowing non-system species assignments when sequence similarity provides strong support. This conservative assignment strategy was chosen because false-positive species detections could lead to overinterpretation of habitat occupancy, whereas genus-level or ambiguous calls still provide useful ecological information without overstating taxonomic certainty. This approach is especially important in species-rich cyprinid assemblages, where closely related taxa may have limited sequence divergence across short mitochondrial amplicons.

Although this 16S assay was adapted from a broad vertebrate primer, a comparable region-specific assessment of expected taxa and marker resolution has not yet been completed for non-Actinopterygii. Therefore, more conservative criteria were applied to non-fish vertebrates. Non-fish vertebrate ESVs were defined as Chordata by Metaworks, excluding Actinopterygii. Primate assignments were treated as human contamination (Homo sapiens). For remaining chordates, species-level calls were accepted only when maximum BLAST identity was ≥98%. Ties meeting this threshold were still assigned to the top hit but exported to a separate review table, retaining the tied-hit species list and identity spread. All other cases (max identity < 98% or missing) were assigned using the most specific MetaWorks classifier rank that met conservative 99%-accuracy bootstrap thresholds (genus ≥ 0.95; family ≥ 0.30).

Partnerships with regional colleagues yielded mitogenomes for Sharpnose and Smalleye shiners at significant cost savings to the project, but resulted in delays (compared with commercial sequencing) for testing original primers and subsequent primer development when existing primers proved to be unreliable, as described above. Development of the new RiVer primer to detect the target species (Sharpnose and Smalleye shiners) and reliably distinguish them from other species in the study system was a necessary delay to genomics processing. Once the new primers were validated, and the genomics pipeline optimized as described above, samples were prepped for bulk sequencing in the UNT Genomics Center. Unfortunately, the MiSeq that was used for our sequencing experienced multiple technical failures at the end of 2025 and during early 2026. Each event required specialized diagnostic and repairs by a ThermoFisher Scientific instrument technician and re-running analyses lost during instrument failure that further delayed sequencing and increased sequencing costs (not billed to the project).

Integration of the eDNA metabarcoding (replicate water samples combined) and seine datasets yielded 568 events with both eDNA and seine data out of a maximum possible 616 events, where possible events is the total number of field sampling events times the number of sites (24 monthly and 4 seasonal sampling events at 22 sites). The lower number of combined samples is due to sites completely or mostly dry that did not have associated eDNA data and/or seine data. The integrated seine and eDNA presence-absence data were arranged into contingency tables for Smalleye and Sharpnose shiners separately (Figure 17), and chi-square analysis was used to test for correlation between seine and eDNA observations. For both species, the largest number of observations fell in the category of absence for both seine and eDNA, but the second largest number of observations was for sites where the species was collected via seining but not detected in the eDNA sampling (Figure 17). Put another way, only 43% (133/309) and 24% (70/290) of the sampling events where Smalleye and Sharpnose shiners, respectively, were collected by seining was the species also registered in eDNA sampling (Figure 16). On comparatively few occasions was either species detected in eDNA samples but not collected by seining (39 for Smalleye and 7 for Sharpnose; Figure 17). Chi-square analyses were significant for both species (Smalleye: $\chi^2 = 52.26$, df = 1, $p < 0.001$; Sharpnose: $\chi^2 = 56.61$, df = 1, $p < 0.001$), indicating that seine and eDNA observations were not correlated.

Given the consistent performance of the new RiVer primer during validation procedures described above, the eDNA false negatives (i.e. species collected in seine sampling but not detected via eDNA) for both species are likely due to inhibition. Environmental conditions such as high temperature, high turbidity, high concentrations of organic compounds (leaf litter, algae) and low pH are known to increase inhibition (e.g. Stoeckle et al. 2017). Those conditions are common in the Upper Brazos River basin (Figure 6), which is why we used Tris-HCl buffer to dilute template DNA and reduce inhibitor concentration. However, it appears that the use of the

buffer alone was insufficient to overcome all sources of inhibition during many collection events. To assess if environmental conditions are likely able to predict under which conditions eDNA suitably replicated traditional seine sampling (i.e. detection with both techniques, vs. eDNA false negatives) we used the environmental PCA (Figure 6) as composite gradients of all instream and riparian habitat conditions and coded samples according to the contingency table for each species (i.e. four categories: seine 1, eDNA 1; seine 1, eDNA 0; seine 0, eDNA 1; seine 0, eDNA 0; Figure 18). Global MANOVAs (multivariate analysis of variance) were significant for both species ($p<0.001$), but post-hoc tests indicated that the global results were driven by higher values on PC1 by the group with no observations via either method (seine 0, eDNA 0; Figure 18). The complete overlap in the ordination space of detection by both methods and eDNA false negatives (Figure 18) demonstrates that eDNA false negatives were observed across a range of environmental conditions observed in the Upper Brazos River and not clearly distinguished from conditions in which both methods detected the target species. Additional experimental research is needed to test field and lab methodologies (e.g. increased sample volume, multi-filter techniques, chemical stripping) that may reduce inhibition further and to refine understanding of ideal conditions for eDNA applications in this and other similar systems.



N. buccula

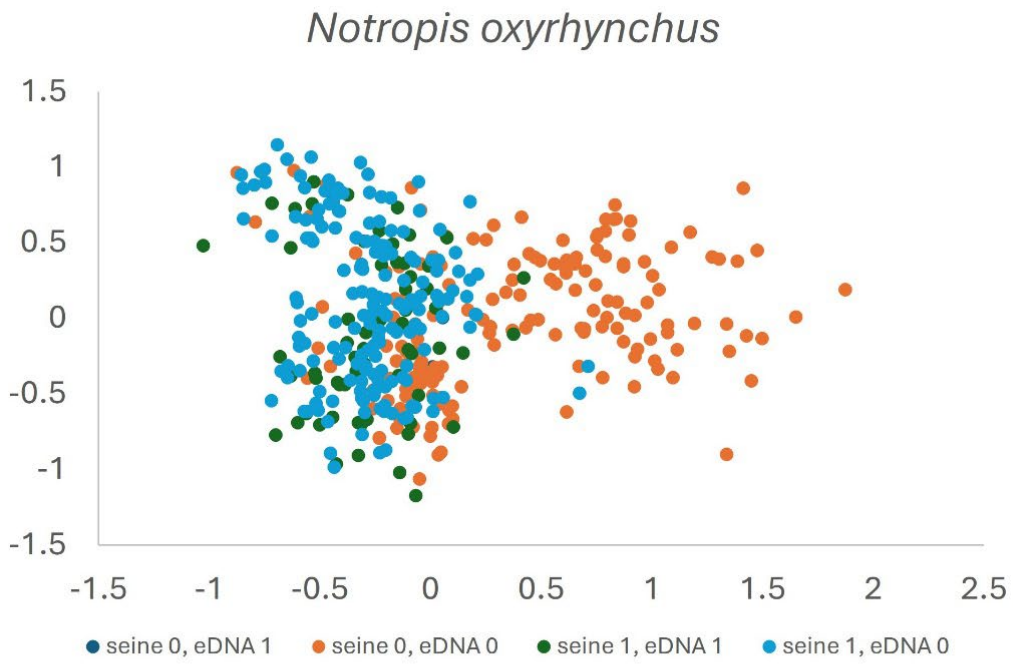
		eDNA	
		1	**0**
seine	**1**	133	176
	0	39	220



N. oxyrhynchus

		eDNA	
		1	**0**
seine	**1**	70	220
	0	7	271

Figure 17: Contingency tables comparing detection (presence-absence) of Smalleye and Sharpnose shiners using standardized seining and eDNA metabarcoding across 22 sites in the Upper Brazos River basin.



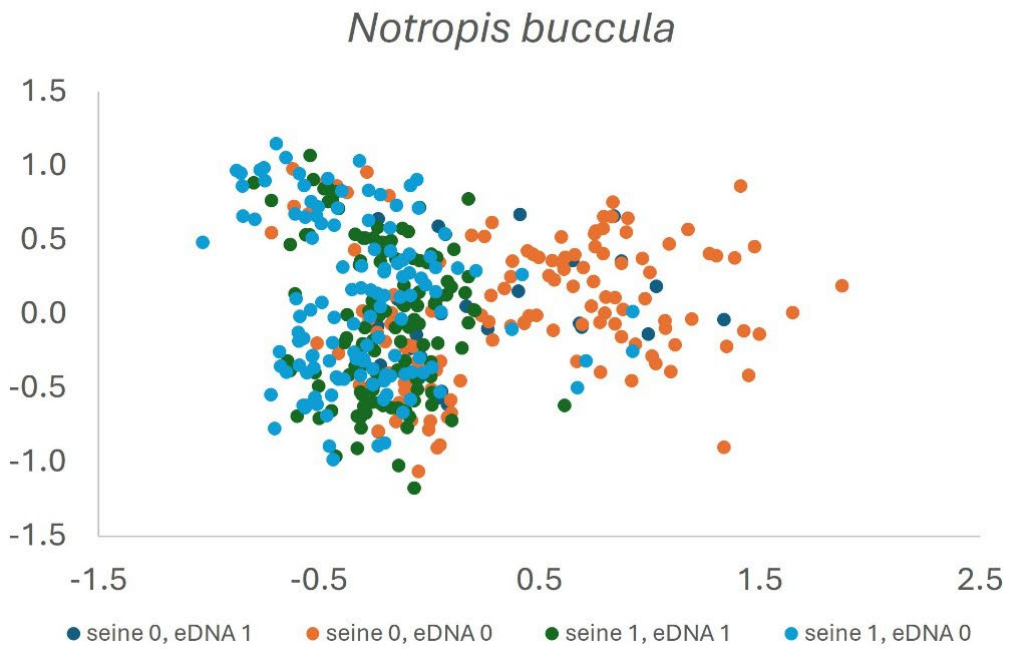


Figure 18: PCA of instream and riparian environmental conditions (see Figure 6) with samples coded based on detection (presence/absence) of each target species via standardized seining and eDNA metabarcoding.

The datasets from standardized seining and eDNA metabarcoding were further integrated to develop a series of occupancy models for Sharpnose and Smalleye shiners to assess: (i) how similar the two methods (seining compared to eDNA metabarcoding) were at shared sites and sampling events for detecting all fish species, (ii) what the eDNA data alone implied about focal-species dynamic occupancy, (iii) what could be inferred when both methods were modeled jointly under a shared latent occupancy state, and (iv) whether ecologically relevant environmental covariates (i.e., flow, depth, and wetted width) improved the integrated focal models. For the metabarcoding data, only records with fish ESV identifiers were retained, meaning that all non-fish vertebrate ESVs and blanks were excluded prior to analyses. Metabarcoding replicates were retained as ordered within-reach sampling positions corresponding to the bottom, middle, and top of each 500-m reach. Note that the seine data was included as a single observation per site/event because individuals collected from each seine haul were not counted separately (i.e. one observation per event for seine vs. 3 observations per event for eDNA). Only exact shared taxa were used for direct cross-method comparisons. All analyses were conducted in the R programing language, with *spOccupancy* package used to conduct occupancy analyses and *coda* used to support posterior and MCMC handling and diagnostics. Method comparisons were performed at two levels. First, shared sampling events were used to compare richness and species overlap between methods. For each shared event, species richness was summarized separately for seine and eDNA detections, and compositional overlap was summarized with the Jaccard index. Second, detections were aggregated to seasonal primary periods to standardize temporal resolution for occupancy modeling and to provide a seasonally comparable view of agreement between methods.

We fit three models for both focal species, *Notropis buccula* and *Notropis oxyrhynchus*: (1) an eDNA-only dynamic occupancy model with constant initial occupancy, colonization, and extinction and with within-reach sample position as a detection covariate (Model 1); (2) an integrated Bayesian occupancy model linking eDNA and seine detections to a shared latent occupancy state with year, season, river-section, and AR(1) temporal structure (Model 2); and (3) an environmental extension of Model 2 that added flow, depth, and wetted width as occupancy covariates (Model 3).

Model 1 was fit with constant colonization and extinction and replicate position as the detection covariate:

$$z_{i,1} \sim Bernoulli(\psi_1)$$
$$z_{i,t} \mid z_{i,t-1} \sim Bernoulli(z_{i,t-1}(1-\varepsilon) + (1 - z_{i,t-1})\gamma), \quad t \geq 2$$
$$y_{i,t,r} \mid z_{i,t} \sim Bernoulli(z_{i,t}\, p_{i,t,r})$$
$$logit(p_{i,t,r}) = \alpha_0 + \alpha_1\, I(Middle_r) + \alpha_2\, I(Upstream_r)$$

where $z_{i,t}$ is the latent occupancy state at site i and season t (1 = occupied, 0 = unoccupied); $y_{i,t,r}$ is the observed eDNA detection/non-detection for replicate r at site i and season t; ψ_1 is the initial occupancy probability in the first primary period; γ is the colonization probability between consecutive primary periods; ε is the extinction probability between consecutive primary periods; $p_{i,t,r}$ is the detection probability for an occupied site in replicate r; and $I(Middle_r)$ and $I(Upstream_r)$ are the indicator variables for eDNA replicate position for the middle and top of the

reach, respectively, with Downstream as the reference level. Although Model 1 captured an important detection pattern, it was not used as the primary inferential model because it relied on eDNA data alone, required a heavily simplified formulation for stable fitting, and the model did not provide the same level of robust uncertainty support as the integrated Bayesian models (Models 2 and 3) which combined both eDNA and seine detections and therefore yielded more defensible estimates of focal-species occupancy through time and across sites.

Model 2 combined eDNA and seine detections under a shared latent occupancy state. Occupancy was allowed to vary through time as a function of centered year, season, river section, and an AR(1) temporal effect; detection was modeled separately for eDNA and seine. Model 2 was defined as follows:

$$z_{i,t} \sim Bernoulli(\psi_{i,t})$$
$$logit(\psi_{i,t}) = \beta_0 + \beta_1\, year_c_{,t} + \beta_2\, spring_t + \beta_3\, summer_t + \beta_4\, fall_t + \beta section(i) + \eta_t$$
$$y^{(E)}_{i,t,r} \mid z_{i,t} \sim Bernoulli(z_{i,t}\, p^{(E)}_{i,t,r})$$
$$logit(p^{(E)}_{i,t,r}) = \alpha_0^{(E)} + \alpha_1^{(E)}\, position_r$$
$$y^{(s)}_{i,t} \mid z_{i,t} \sim Bernoulli(z_{i,t}\, p^{(s)}_{i,t})$$
$$logit(p^{(s)}_{i,t}) = \alpha_0^{(s)}$$
$$\eta_t = \rho\, \eta_{t-1} + \omega_t, \quad \omega_t \sim Normal(0, \sigma^2_t)$$

where $\psi_{i,t}$ is occupancy probability at site i and season t; $year_c_{,t}$ is the centered year covariate; $spring_t$, $summer_t$, $fall_t$ are the seasonal indicator variables, with winter as the reference season; $\beta section(i)$ is the effect of river section (River Fork grouping) for site i; $y^{(E)}_{i,t,r}$ is the eDNA detection/non-detection observation; $y^{(s)}_{i,t}$ is the seine detection/non-detection observation; $p^{(E)}_{i,t,r}$ is eDNA detection probability; $p^{(s)}_{i,t}$ is the seine detection probability; $position_r$ is the within-reach eDNA sampling position (Downstream, Middle, and Upstream sampling location of the reach), with Downstream as the reference level; η_t is the temporal random effect, AR(1); ρ is the temporal autocorrelation parameter; and σ^2_t is the variance term for the temporal process.

Model 3 followed same structure as Model 2, but flow, depth, and wetted width were added as occupancy covariates; these variables were standardized and used in the occurrence component of the model, but not the detection component. Model 3 was defined as:

$$z_{i,t} \sim Bernoulli(\psi_{i,t})$$
$$logit(\psi_{i,t}) = \beta_0 + \beta_1\, year_c_{,t} + \beta_2\, spring_t + \beta_3\, summer_t + \beta_4\, fall_t + \beta_5\, flow_{i,t} + \beta_6\, depth_{i,t} + \beta_7\, ww_{i,t} + \beta section(i) + \eta_t$$
$$y^{(E)}_{i,t,r} \mid z_{i,t} \sim Bernoulli(z_{i,t}\, p^{(E)}_{i,t,r})$$
$$logit(p^{(E)}_{i,t,r}) = \alpha_0^{(E)} + \alpha_1^{(E)}\, position_r$$
$$y^{(s)}_{i,t} \mid z_{i,t} \sim Bernoulli(z_{i,t}\, p^{(s)}_{i,t})$$
$$logit(p^{(s)}_{i,t}) = \alpha_0^{(s)}$$
$$\eta_t = \rho\, \eta_{t-1} + \omega_t, \quad \omega_t \sim Normal(0, \sigma^2_t)$$

where $flow_{i,t}$ is the standardized flow covariate for site i and season t; $depth_{i,t}$ is the standardized depth covariate for site i and season t; $ww_{i,t}$ is the standardized wetted-width covariate for site i and season t; β_5, β_6, β_7 are the regression coefficients for flow, depth, and wetted width, respectively; and all other variables are as defined for Model 2 above.

Models 2 and 3 were compared with weighted AIC (WAIC), and posterior summaries of z were used to describe inferred site- and season-specific occupancy, whereas psi was retained as the modeled occupancy surface implied by the occurrence model.

Across shared sampling events, eDNA recovered more shared taxa per event than seining on average (mean 3.90 vs. 2.48 shared taxa; Figure 19), and mean Jaccard overlap was moderate (0.34), indicating partial but not complete concordance between methods. Jaccard overlap was highest in fall and lowest in winter, suggesting that agreement varied seasonally (Figure 20). Species-level agreement was highest for common shared taxa, such as *Cyprinella lutrensis*, *Fundulus zebrinus*, and *Hybognathus placitus*, whereas several taxa showed little or no overlap between methods despite occasional detection by one method or the other (Figure 21). For the focal species, sampling event agreement was relatively low (Figure 22).

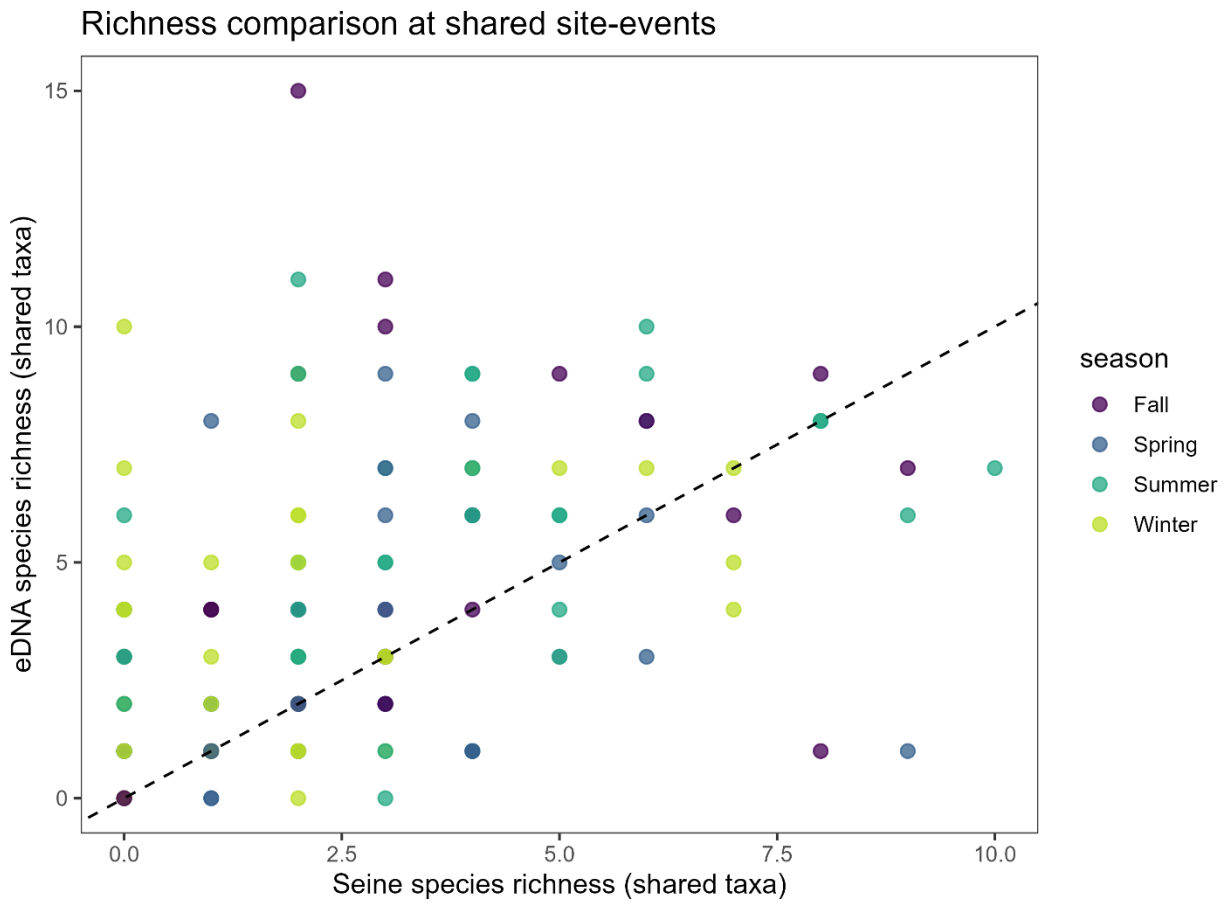


Figure 19: Event-level richness comparison for shared taxa between eDNA and seining. eDNA generally recovered more shared taxa per event than seining.

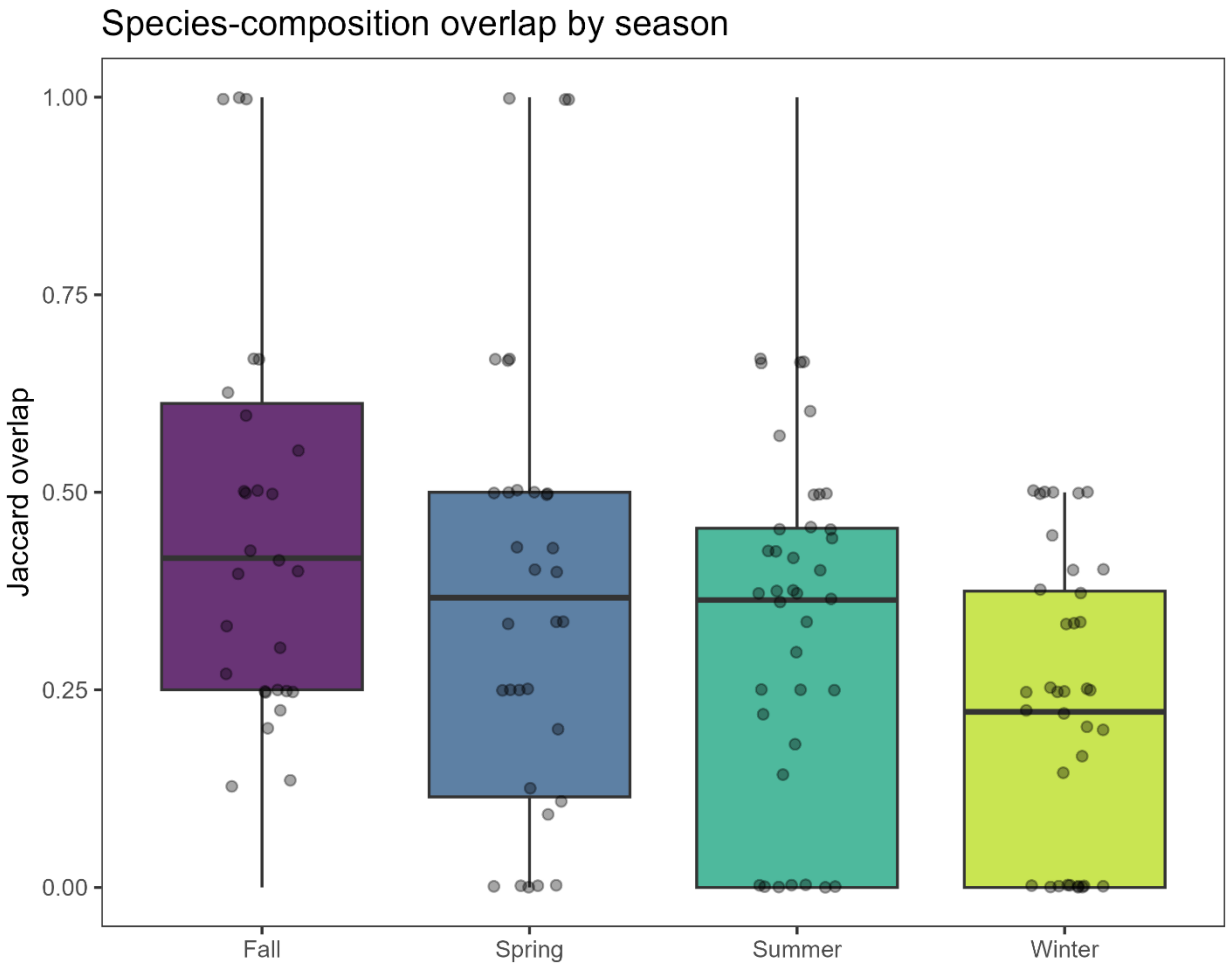


Figure 20: Season-specific distribution of Jaccard overlap across shared events. Overlap was moderate overall and varied seasonally.

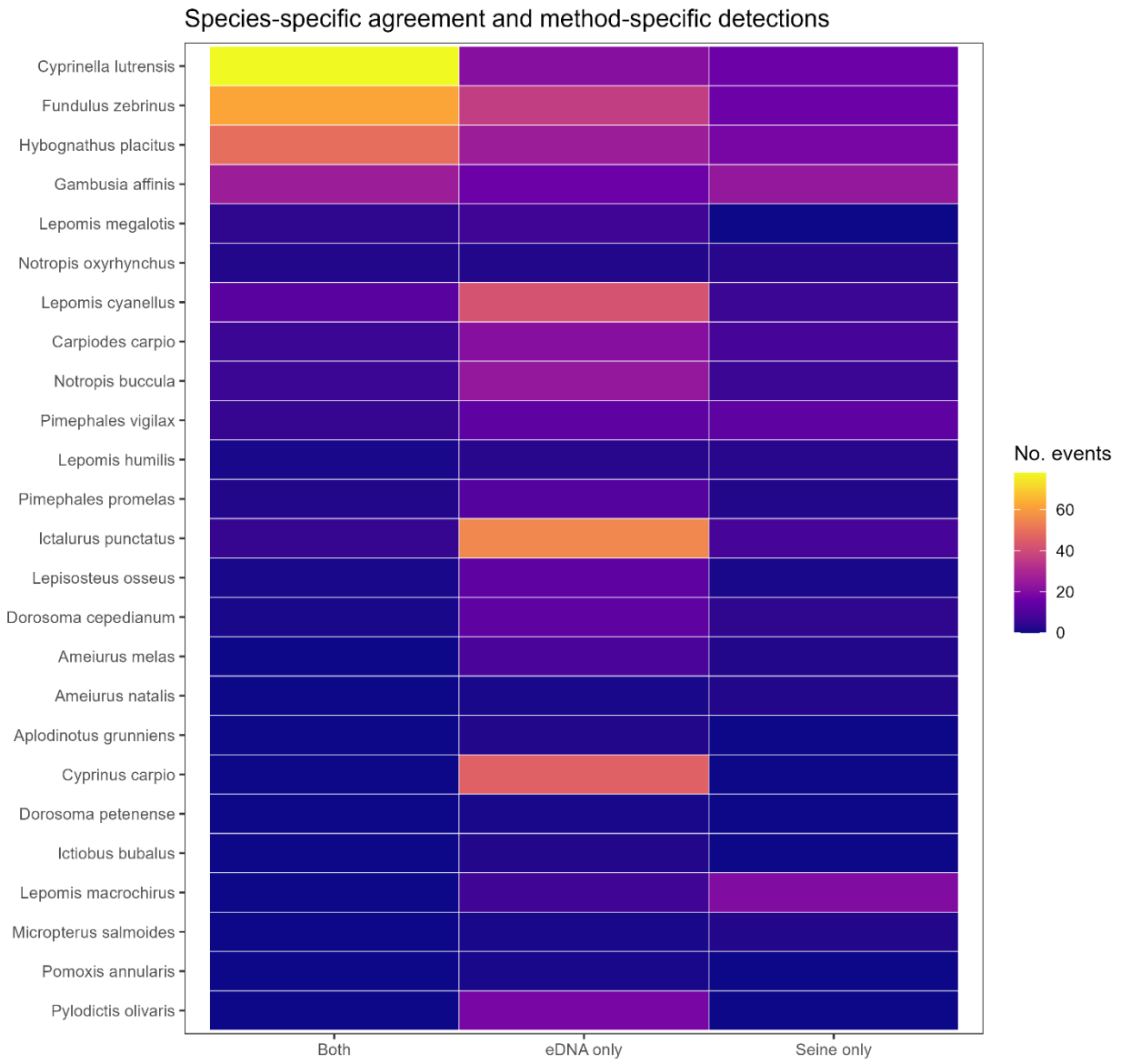


Figure 21: Species-specific counts of shared detections, eDNA-only detections, and seine-only detections. Agreement was highest for common shared taxa and lower for rare taxa.

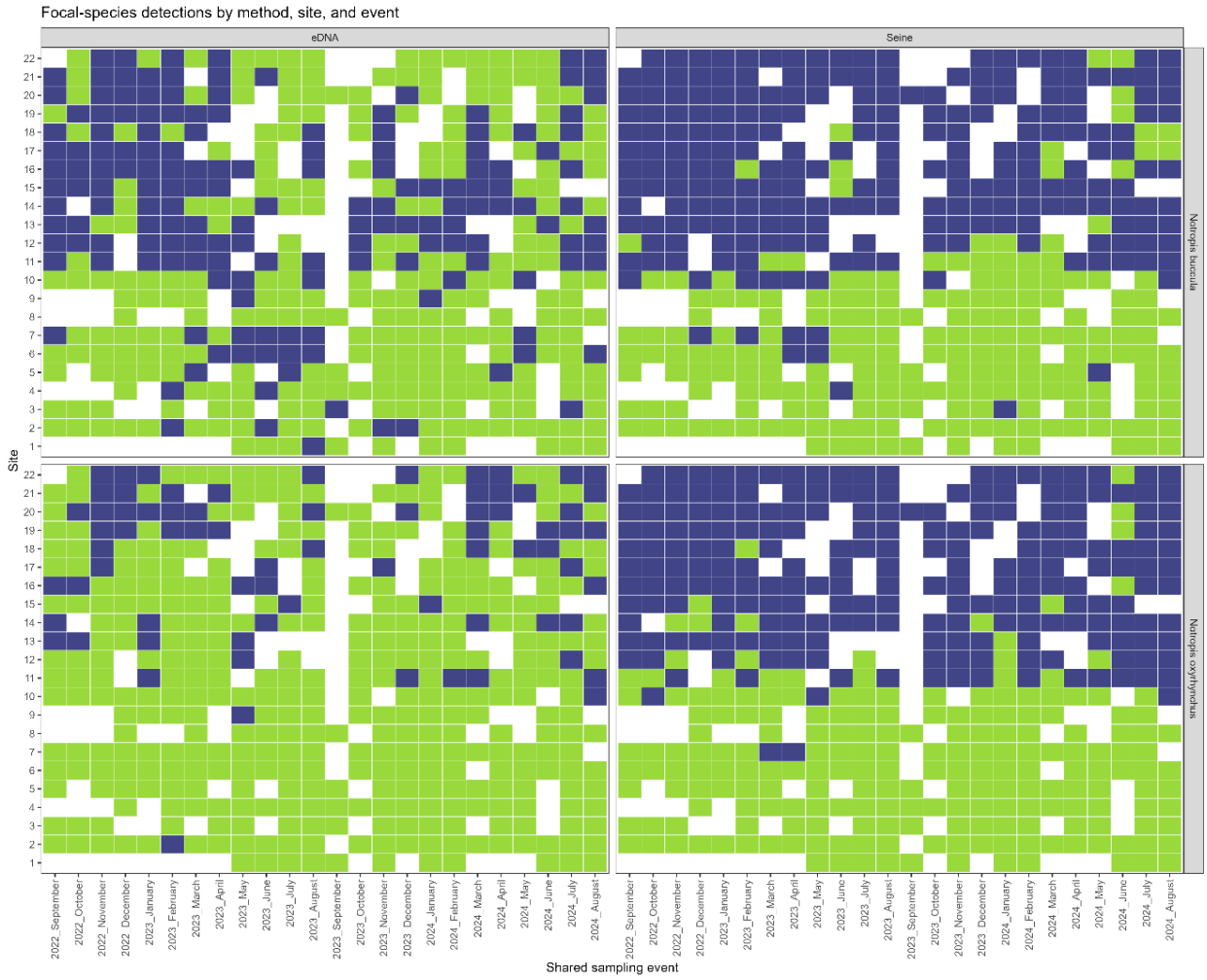


Figure 22: Focal species (*Notropis buccula* top panels, and *Notropis oxyrhynchus* bottom panels) by sampling method (eDNA left panels, and seine right panels) and shared monthly sampling period. Green squares indicate no detections and blue squares indicate detections.

The eDNA-only dynamic occupancy model (Model 1) indicated that detection probability varied strongly with within-reach sampling position, with Upstream (top of reach) and Middle (mid-reach) samples outperforming Downstream (bottom of reach) samples for both focal species (Table 1). For *Notropis buccula*, the fitted eDNA-only model suggested moderate initial occupancy and very high colonization with low extinction, whereas for *N. oxyrhynchus* the model returned extremely low initial occupancy and very low baseline detection, consistent with the rarity of this species in the eDNA dataset. As stated above, Model 1 was not used as the primary inferential model because it relied on eDNA data alone, required a heavily simplified formulation for stable fitting, and the model did not provide the same level of robust uncertainty support as the integrated Bayesian models (Models 2 and 3) which combined both eDNA and seine detections and therefore yielded more defensible estimates of focal-species occupancy through time and across sites.

Integrated baseline models (Model 2) for both focal species converged on the same retained structure (Table 2). For *N. buccula*, the centered year effect was credibly positive (1.62 [0.42, 3.05]), whereas spring, summer, fall, and river-section contrasts all had 95% credible intervals overlapping zero (Table 2). For *N. oxyrhynchus*, the year effect was also credibly positive (1.59 [0.69, 2.75]), and summer was additionally positive relative to the reference season (1.85 [0.23, 3.55]), while river-section contrasts remained uncertain (Table 2). For both species, eDNA detection increased with within-reach position (from downstream to upstream), and the seine detection intercept remained lower than the eDNA position effect, reinforcing the value of replicated eDNA sampling for the focal taxa. Note that this result is almost certainly due to the single observation from pooled seine hauls in comparison with three replicates for eDNA, rather than a meaningful increase in detection probability from eDNA vs. seining. This interpretation is supported by the very large number of false negatives in the eDNA dataset (Figures 17 and 22).

Integrated environmental models (Model 3; Table 3) converged for both species, but model comparison favored the baseline integrated model (Model 2) in both cases (Table 4). For *N. buccula*, baseline WAIC was 792.78 versus 794.13 for the environmental model (ΔWAIC = +1.35, environmental minus baseline), and for *N. oxyrhynchus* baseline WAIC was 442.81 versus 447.34 for the environmental model (ΔWAIC = +4.53), indicating worse predictive fit after adding flow, depth, and wetted width. Environmental effects were directionally mixed but uncertain: for *N. buccula*, flow was weakly positive (0.17 [-1.25, 1.60]), depth was weakly negative (-0.44 [-1.33, 0.55]), and wetted width was weakly positive (0.39 [-0.64, 1.44]); for *N. oxyrhynchus*, all three effects also overlapped zero. Again, it is important to keep in mind that these models reflect the data structure of replicated eDNA samples at each site with a single seine observation. Thus, these results do not contradict the estimates of high-quality habitat based on integrated thresholds presented above or suggest that eDNA has higher detection probability for the focal taxa – rather the models take advantage of the additional eDNA observations to improve model fit, but this results in a greater relative weight of eDNA to seine data in the model structure. Results from these occupancy analyses suggest that eDNA and seining are complementary rather than interchangeable for the focal taxa and the upper Brazos river system. The replicated eDNA design appears to have delivered more information on detection, which likely improved the ability of the integrated models to estimate occupancy for both focal species – similar gains could be achieved by recording data from individual seine hauls as replicates, though this is less feasible in practice.

Posterior z summaries did not substantially change between the baseline (Model 2) and the environmental (Model 3) integrated models (Table 5, Figures 23 and 24). For *N. buccula*, mean posterior occupancy across seasons rose slightly from 0.872 in the baseline model (Model 2) to 0.885 in the environmental model (Model 3), with the lowest value in winter 2022 and the highest in summer 2025 in both model sets (Table 5). For *N. oxyrhynchus*, mean posterior occupancy across seasons increased from 0.608 for the baseline model (Model 2) to 0.638 for the environmental model (Model 3), but the same qualitative pattern persisted: low occupancy in winter 2022 and high occupancy by summer 2025 (Table 5). Thus, the environmental covariates altered the fitted surface only modestly and did not change the central temporal signal. Both focal species showed positive year effects in the integrated models (Model 2), and posterior z trajectories indicate especially high occupancy by 2024–2025 relative to early 2022, possibly indicating recovery of the focal species from extreme drought at the beginning of the study. This pattern of increasing detectability through time was particularly striking for *N. oxyrhynchus*,

which was rare in the raw detection tables but still showed a coherent increase through time once imperfect detection was modeled explicitly. This result underscores the value of the integrated occupancy framework: it can recover plausible underlying occupancy dynamics even when one or both data sources are sparse.

The integrated environmental models (Model 3) were informative for both focal *Notropis* species, even though they were not preferred. Flow, depth, and wetted width are ecologically reasonable covariates for both focal species, but at the scale and resolution used here they did not improve predictive fit, and all three posterior intervals overlapped zero for both species. That result can be interpreted in several, non-exclusive ways. First, the main signal may already be captured by broad temporal structure and river section. Second, while using site means (rather than 5 transects per site) for environmental data is necessary to apply to both seine and eDNA data, it does not achieve the biological scale of the eDNA replicates which contribute most to occupancy due to the larger number of observations.

Table 1. Back-transformed parameter estimates for the eDNA-only focal dynamic occupancy models (Model 1). Detection probabilities are shown for each eDNA sampling position within the reach.

Species	ψ_1	γ	ε	p(Downstream)	p(Middle)	p(Upstream)
Not buc	0.316	0.999	0.003	0.162	0.451	0.467
Not oxy	<0.001	0.317	<0.001	0.006	0.169	0.426

Table 2. Results for the integrated baseline model without environmental covariates (Model 2).

Species	Year effect	Spring	Summer	Fall	River section effects	eDNA position	Seine intercept	AR1 rho
Not buc	1.62 [0.42, 3.05]	1.91 [-0.51, 4.44]	1.69 [-0.05, 3.68]	0.82 [-0.93, 2.63]	All 95% CrIs overlap 0	0.73 [0.49, 0.97]	-1.39 [-1.94, -0.87]	-0.12 [-0.95, 0.93]
Not oxy	1.59 [0.69, 2.75]	0.70 [-0.93, 2.35]	1.85 [0.23, 3.55]	0.47 [-1.23, 2.20]	All 95% CrIs overlap 0	1.73 [1.32, 2.17]	-1.40 [-2.30, -0.57]	-0.22 [-0.89, 0.73]

Table 3. Results for the integrated baseline model without environmental covariates (Model 3).

Species	Year effect	Spring	Summer	Fall	Flow	Depth	WW	River section effects	eDNA position	Seine intercept	AR1 rho
Not buc	1.80 [0.47, 3.23]	2.37 [-0.15, 5.00]	1.90 [-0.06, 4.15]	0.82 [-1.08, 2.80]	0.17 [-1.25, 1.60]	-0.44 [-1.33, 0.55]	0.39 [-0.64, 1.44]	All 95% CrIs overlap 0	0.71 [0.47, 0.95]	-1.42 [-1.96, -0.91]	-0.07 [-0.97, 0.90]
Not oxy	1.92 [0.85, 3.21]	0.83 [-1.04, 2.66]	2.06 [0.27, 4.02]	0.63 [-1.20, 2.51]	-0.30 [-1.28, 0.71]	-0.32 [-1.12, 0.45]	-0.04 [-0.78, 0.72]	All 95% CrIs overlap 0	1.70 [1.28, 2.13]	-1.49 [-2.37, -0.63]	-0.20 [-0.92, 0.86]

Table 4. Baseline (Model 2) vs environmental (Model 3) integrated-model comparison.

Species	Baseline integrated model (Model 2)	Environmental integrated model (Model 3)	Baseline WAIC	Environmental WAIC	ΔWAIC (env-baseline)	Preferred model	Flow effect mean	Depth effect mean	Wetted width effect mean
Not buc	season_year_riversection_ar1	season_year_env_riversection_ar1	792.783	794.134	1.351	Model 2	0.167	-0.442	0.385
Not oxy	season_year_riversection_ar1	season_year_env_riversection_ar1	442.812	447.34	4.528	Model 2	-0.299	-0.320	-0.038

Table 5. Posterior z summary of baseline (Model 2) compared to environmental (Model 3) integrated models.

Species	Model 2 mean z across seasons	Model 3 mean z across seasons	Model 2 lowest season	Model 3 lowest season	Model 2 highest season	Model 3 highest season	Model 2 lowest site	Model 3 lowest site	Model 2 highest site	Model 3 highest site
Not buc	0.872	0.885	2022_Winter (0.38 [0.18, 0.73])	2022_Winter (0.41 [0.18, 0.77])	2025_Summer (0.99 [0.95, 1.00])	2025_Summer (1.00 [0.95, 1.00])	Site 18 (0.73 [0.47, 0.93])	Site 20 (0.77 [0.60, 0.93])	Site 8 (0.99 [0.93, 1.00])	Site 8 (0.99 [0.93, 1.00])
Not oxy	0.608	0.638	2022_Winter (0.07 [0.00, 0.27])	2022_Winter (0.09 [0.00, 0.32])	2025_Summer (0.95 [0.77, 1.00])	2025_Summer (0.97 [0.82, 1.00])	Site 18 (0.43 [0.20, 0.67])	Site 18 (0.48 [0.27, 0.73])	Site 3 (0.82 [0.60, 1.00])	Site 3 (0.85 [0.67, 1.00])

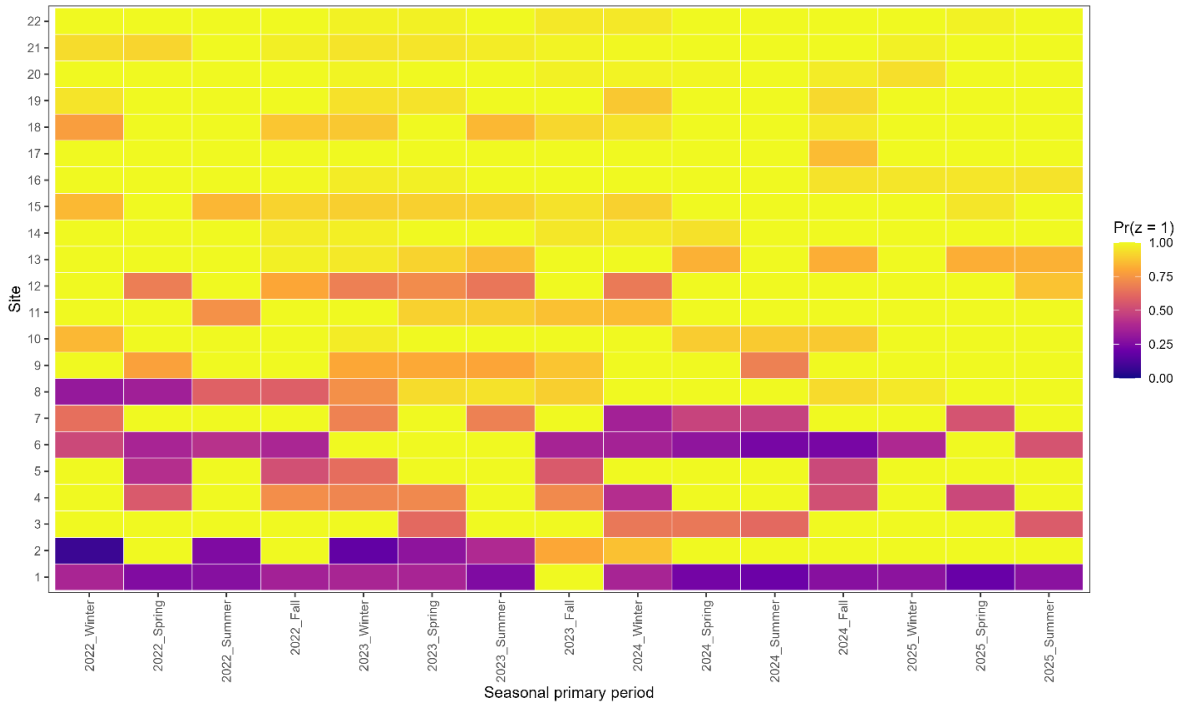


Figure 23: Integrated posterior occupancy scores (z) for *Notropis buccula* for the base model (Model 2). Occupancy was much higher in the main stem sites across all seasons.

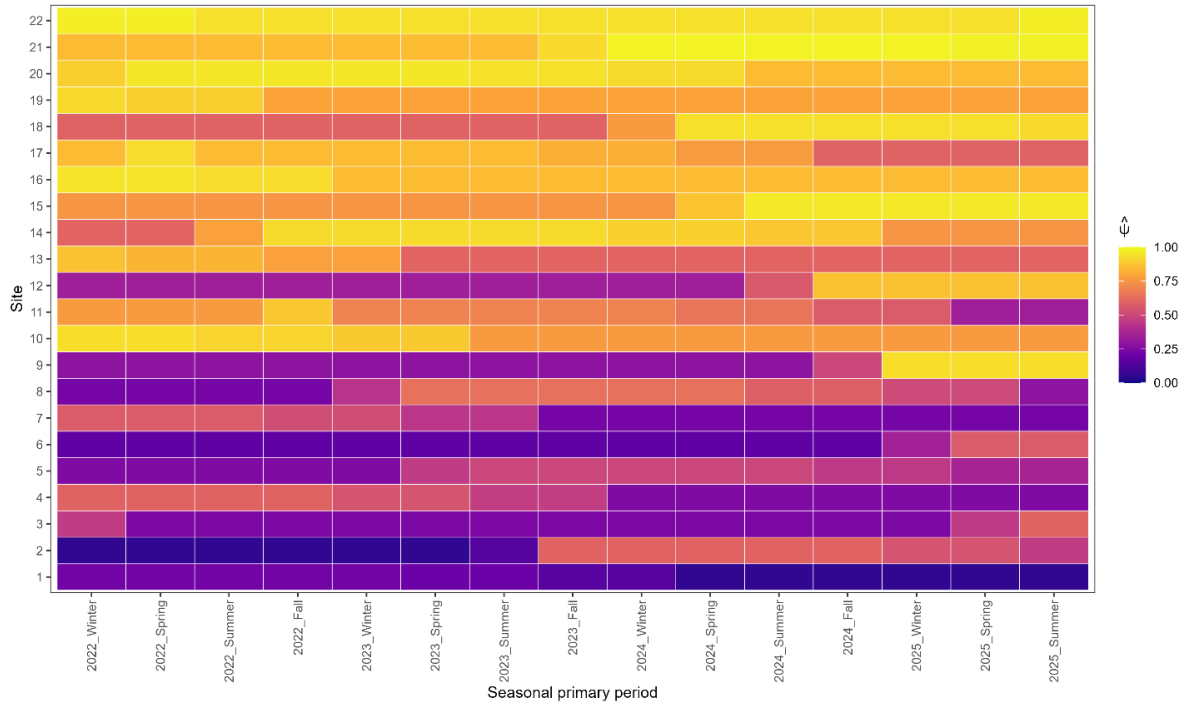


Figure 24: Integrated posterior occupancy scores (z) for *Notropis oxyrhynchus* for the base model (Model 2). Occupancy was much higher in the main stem sites across all seasons.

In addition to primer development and assessment of eDNA metabarcoding for Sharpnose and Smalleye shiners, we also developed and validated field-deployable, loop-mediated isothermal amplication (LAMP) assays (Notomi et al. 2000) for both target species. LAMP assay development was pursued as a complementary tool to DNA metabarcoding because it offers the potential for rapid, species-specific detection outside of a sequencing workflow. While metabarcoding is well-suited for broad community assessment, LAMP assays can be used to provide same-day, point-of-use information about whether target species DNA is present in environmental samples. This made LAMP assays compelling as an approach for evaluating whether a portable molecular assay could support rapid detection of the focal shiner species during field surveys.

Assay design leveraged newly available complete mitochondrial genomes for both species generated from vouchered specimens collected in Baylor and Knox counties in the upper Brazos River (Fields et al. 2024). The use of complete mitochondrial genomes from vouchered Upper Brazos specimens was critical because the focal species occur in a taxonomically challenging assemblage that includes closely related cyprinids. Locally derived reference genomes reduced the risk of designing assays around sequence variants that were not representative of the study system and allowed candidate LAMP regions to be evaluated across the full mitochondrial genome, rather than being constrained to a single, short marker region. This was especially important for identifying genomic regions that were conserved within each target species but divergent from closely related, non-target taxa.

LAMP is an isothermal nucleic-acid amplification approach that uses multiple primers recognizing distinct target sites, providing high specificity and rapid amplification under constant temperature conditions (Notomi et al. 2000; Nagamine et al. 2002). Because LAMP reactions rely on multiple primers binding to the same target region, they can be highly specific when primer sets are well designed. However, this same multi-primer structure also makes careful assay screening essential, particularly for closely related species that may share substantial mitochondrial sequence similarity. For this reason, our workflow combined in silico primer discovery, BLAST-based specificity screening, mismatch evaluation at key priming sites, laboratory optimization, and field validation against conventional sampling.

Reference sequence curation and alignment: For each target species, available mitochondrial genome sequences were compiled. Reference sequence curation followed a standardized assay-design workflow. Available complete mitochondrial sequences were retrieved and organized in Geneious Prime, then aligned using MUSCLE to compare sequence variation among available records. A representative mitogenome was selected for each species based on low divergence relative to the alignment, thereby reducing the likelihood that primer design would be based on an unusual or highly divergent sequence variant. Because PrimerExplorer V5 accepts target sequences up to 2,000 bp, the selected template mitogenome was partitioned into sequential 2,000 bp windows for primer discovery. Partitioning the mitogenome into sequential windows allowed primer discovery to proceed across the full mitochondrial genome, rather than focusing only on commonly used barcode regions. This increased the likelihood of identifying short regions that met the technical requirements for LAMP amplification while also containing sequence differences useful for discriminating the focal species from congeners and other closely related taxa. When insufficient candidate assays were identified within the initial windows, overlapping windows were evaluated across window boundaries to avoid missing suitable primer regions that spanned arbitrary 2,000-bp breaks.

Primer discovery using PrimerExplorer V5: Candidate LAMP primer sets were generated in PrimerExplorer V5 (Eiken Chemical Co., Ltd.) by uploading each 2,000 bp window and producing candidate primer sets (F3, B3, FIP, BIP). For each 2,000-bp input sequence, PrimerExplorer generated up to five candidate primer sets, which were reviewed in the order recommended by the software. Primer information files and primer sequence files were saved for each candidate set so that candidate assays could be revisited, loop primers could be generated, and primer sequences could be transferred into downstream screening and documentation files. Candidate sets were retained for downstream consideration only when both loop primers (LF and LB) were available after PrimerExplorer filtering, because loop primers can improve reaction speed and robustness (Nagamine et al. 2002). Requiring both forward and backward loop primers provided an additional screening step before laboratory testing. Primer sets lacking either LF or LB were deprioritized because they were expected to be less useful for rapid field detection, where faster amplification and robust performance are important. When multiple, highly similar loop-primer options were available for a candidate assay, the highest-ranked PrimerExplorer option was retained for downstream screening.

In silico specificity screening and mismatch assessment: For each viable primer set, the full target region spanning F3 to B3 was extracted and screened using NCBI Nucleotide BLAST to identify potential non-target matches. BLAST screening was used as an initial specificity filter rather than as the sole basis for assay acceptance. Candidate assays were flagged for further review when the F3–B3 target region returned high-similarity matches to non-target species, particularly other *Notropis* or cyprinid taxa expected to occur in the region. Assays were prioritized when the 1) target species was clearly the best match, 2) non-target alignments showed mismatches in primer-binding regions likely to reduce amplification, and 3) candidate regions showed comparatively low similarity to closely related *Notropis* taxa. To further increase discrimination among closely related taxa, we performed an in silico mismatch assessment at the putative priming sites most influential to amplification (F2 and B2 regions within the FIP and BIP primers). Particular attention was given to the F2 and B2 regions because these sequences are embedded within the inner primers and are central to initiating LAMP amplification. Candidate assays were favored when mismatches to non-target taxa occurred near the 3′ ends of these key priming regions, because such mismatches are more likely to reduce extension and therefore reduce the probability of non-target amplification. This mismatch-based prioritization was especially important because the target species are closely related to other regional cyprinids. Furthermore, primer sets were prioritized when they were fully conserved within the target species and contained 3'-proximal mismatches in closely related non-target taxa expected to reduce non-target amplification. The final list of all the sequences tested and the top candidate LAMP target regions can be found in the supplemental Excel file, "Brazos LAMP Target Regions.xlsx", under the "Sequences_Tested" and "Top_Target_Regions" tabs, respectively.

Assay transfer, primer screening, and optimization: Following in silico selection of target regions by our laboratory, target regions were provided to Agdia (Bryant Davenport) for primer testing, optimization, and validation in the lab (Table 6). Compson's laboratory was responsible for reference sequence curation, genome-wide candidate region identification, in silico specificity screening, and prioritization of candidate target regions. Agdia then performed laboratory testing of selected candidate assays, including empirical primer screening (Tables 7 and 8), optimization of reaction conditions, evaluation of background amplification, and formulation of the final assays into field-deployable lyophilized pellets.

Table 6. Summary of laboratory optimization and validation stages.

Stage	Input material	Key comparisons	Run format / readout	Core parameters	Primary acceptance / interpretation
Primer screening	Target DNA; NTCs	2 primer sets per species	AmplifyRP XRT; AmpliFire (FAM)	Isothermal incubation (screening runs)	Select candidates for optimization; monitor NTC behavior
Optimization	Target DNA; NTCs; cross-reactor DNA	Temperature evaluation; primer titration when NTC signal present	AmplifyRP XRT; AmpliFire (FAM)	Species-specific temperature refinement	Reduce background/NTC amplification; improve specificity
Lot-level QC (Pellet lot 101525)	Serially diluted target DNA; NTCs; cross-reactors	Ten-fold dilution series; cross-reactor panel	AmplifyRP XRT; AmpliFire (FAM)	5 µL sample + 100 µL PD2; 25 µL to pellet; 40 min at 68 °C (*N. buccula*) or 67 °C (*N. oxyrhynchus*)	Pass if detects through 1:10,000 and NTC/cross-reactors negative

After receiving the target regions from our lab, Agdia initially screened two candidate primer sets per species (Tables 7 and 8) against target DNA and non-template controls (NTCs). Candidate assays were advanced when they showed rapid and repeatable amplification of target DNA, no amplification or substantially delayed amplification in non-template controls, and improved discrimination between target and non-target DNA during optimization. Assays that produced background signal or inconsistent amplification were either modified through primer concentration adjustments and temperature optimization or were deprioritized. Optimization focused on reducing NTC/background amplification (including primer titration when NTC signal was observed), and improving analytical specificity using temperature evaluation across a small range of isothermal incubation temperatures. Optimized assays were subsequently formulated as lyophilized reaction pellets suitable for portable field-forward workflows.

Reaction format and run conditions: Quality-control testing and subsequent validation were performed in the AmplifyRP XRT format and interpreted on an AmpliFire isothermal fluorometer with fluorescence measured in the FAM channel. The lyophilized pellet format was selected to simplify field deployment by reducing the number of liquid reagents that needed to be handled on site and by standardizing reaction chemistry across runs. Use of the Agdia's AmpliFire isothermal fluorometer allowed reactions to be incubated and interpreted under controlled temperature conditions without requiring a conventional thermocycler, making the workflow suitable for mobile or field-forward testing. In Agdia's QC workflow, DNA templates were serially diluted in water and pellets were equilibrated to room temperature. A pre-dispensed Tris diluent (PD2; 25 mM Tris) was used by adding 5 µL of diluted template to 100 µL PD2, mixing, and then adding 25 µL of the PD2/sample mixture to rehydrate a lyophilized pellet. Reactions were run for 40 minutes at 68 °C for the *N. buccula* assay and 67 °C for the *N. oxyrhynchus* assay, unless otherwise specified during optimization.

Table 7. LAMP oligos designed for *N. oxyrhynchus* based on sequences shared with Agdia. Oligos highlighted in green were selected for ordering and evaluation. The final selected primers are highlighted in green AND in bold (set 5).

Set	Primer	Sequence (5'-3')	Target
1	F3	GGGTTCATGCCGAAGTGG	*Notropis oxyrhynchus*
	B3	GGCTTGAGTTGTCTGGGC	*Notropis oxyrhynchus*
	FIP	TAATCAGGGCGGCAAGAGCC GGAACTAGCAAACCAAGGCC	*Notropis oxyrhynchus*
	BIP	ACTTGCGACTCTGCTACGCAA TCAAGGGGTAGATGAGGTGA	*Notropis oxyrhynchus*
2	F3	GGGCACCCTTTGACCTAAC	*Notropis oxyrhynchus*
	B3	GGATAAGAGGGCGGCTTTG	*Notropis oxyrhynchus*
	FIP	GGCGTACTCGGCGAGGAAAAAT TGTCTCAGGCTTCAATGTCG	*Notropis oxyrhynchus*
	BIP	CCTCTCCGCCGTGCTGTTTT TGTGGTGAGCTCGGGTAC	*Notropis oxyrhynchus*
	LF	AAGGGGCCCCCTGCATA	*Notropis oxyrhynchus*
	LB	TGGGAACATCTTACTTTCCAGCC	*Notropis oxyrhynchus*
3	F3	CCGCCCTGGTGTTACTA	*Notropis oxyrhynchus*
	B3	CTTGAGTTGTCTGGGCTC	*Notropis oxyrhynchus*
	FIP	GTTGCAGTAAGAGGGAGGCCT CTCCCCCCACTCACC	*Notropis oxyrhynchus*
	BIP	GCTCTTGCCGCCCTGATT GGAAATGGTGAGAGTTATTGC	*Notropis oxyrhynchus*
	LF	ACCACTTCGGCATGAACCC	*Notropis oxyrhynchus*
	LB	GCCTGTACTTTTACTTGCGACTCTG	*Notropis oxyrhynchus*
4	F3	GCAAGCACAACTAATGCATG	*Notropis oxyrhynchus*
	B3	CCAAGGGCTGTGAGAAG	*Notropis oxyrhynchus*
	FIP	CATTCAGAAATGCATCGGCGC GACCCAATTGCTACTGCC	*Notropis oxyrhynchus*
	BIP	CCCGAGGTTCTACAGGGATTAGAT TTGAACAATTAGGGCGAATG	*Notropis oxyrhynchus*
	LF	CCAATCTTCAGCGCCAGGG	*Notropis oxyrhynchus*
5	**F3**	**CTCTCTAAAGAGCTTATCTACCC**	***Notropis oxyrhynchus***
	B3	**GAATAGTATGGAGGATACTAGGC**	***Notropis oxyrhynchus***
	FIP	**CTCACTGAGGAGTATGCAATTAGCG TTATTATCTTAGCACTCTGGGG**	***Notropis oxyrhynchus***
	BIP	**GGCCTTGTAGCAGGCGGA CGTGGGCGATTATAAGGATA**	***Notropis oxyrhynchus***
	LF	**TTGGCGAAGACAAATAGACCCTG**	***Notropis oxyrhynchus***
	LB	**CCAAACTCCGTGGGGATTCTCG**	***Notropis oxyrhynchus***
	Probe	**CATCCGCATTCGCATCCGGGTCCTCAGCGT/36-FAM/**	**N/A**
	Quencher	**/5IABkFQ/ACGCTGAGGACCCGGATGCGAATGCGGATGCCAAACTCCGTGGGGATTCTCG**	***Notropis oxyrhynchus***

Table 8. LAMP oligos designed for *N. buccula* based on sequences shared with Agdia. Oligos highlighted in blue were selected for ordering and evaluation. The final selected primers are highlighted in blue AND in bold (set 2).

Set	Primer	Sequence (5'-3')	Target
1	F3	CCCCTCGCAGAACAGAGAA	*Notropis buccula*
	B3	ACTTGGGGGGGATGTTGG	*Notropis buccula*
	FIP	TGGTGGTGATGGGGGGATTGT CATCAATGGCTGCCCAAGAA	*Notropis buccula*
	BIP	GCACGTACCCCATTACCGAGC GTATTTGCGTACTCGGCA	*Notropis buccula*
	LF	TGAGGGGGGTGACATGAGG	*Notropis buccula*
	LB	CTTCCCCAGGCCTCTGGAA	*Notropis buccula*
2	**F3**	**GGTATGAACAACTGCCGCTG**	***Notropis buccula***
	B3	**CCTGCAGTGAAGTGAGAAGT**	***Notropis buccula***
	FIP	**TCTGTGGCCAAGTAGGCATTGG CTTGCAAGCCTCACTTGGTT**	***Notropis buccula***
	BIP	**AGTGTTGACATGCTGGCTCCTC GTGCAATAGGCTCAGGGTTA**	***Notropis buccula***
	LF	**CCGGTCTCTGAAGTTCAGCC**	***Notropis buccula***
	Probe	**CATCCGCATTCGCATCCGGGTCCTCAGCGT/36-FAM/**	**N/A**
	Quencher	**/5IABkFQ/ACGCTGAGGACCCGGATGCGAATGCGGATGCCGGTCTCTGAAGTTCAGCC**	***Notropis buccula***
3	F3	ATTGTATGGGCCCACCAT	*Notropis buccula*
	B3	AACAATCCCTGTTAGTCCA	*Notropis buccula*
	FIP	GCAATAATCATTGTTGCAGATGTGA ATGTTTACTGTTGGAATAGACG	*Notropis buccula*
	BIP	CACTCCACGGAGGCTCAATT CAACTGTAAAGAGGAAAATAAAGC	*Notropis buccula*
	LB	ACTCCAATGCTATGGGCCCTAG	*Notropis buccula*
4	F3	CCGAGGTGATGCAAGGATT	*Notropis buccula*
	B3	TGCGATTGAGGAGTAGGCT	*Notropis buccula*
	FIP	ATAAGGGCAAGCGGGGCAAG AGACTTGCTGACGGGATTG	*Notropis buccula*
	BIP	TCCTTCTCACATCCCTCGGACT TCCGCAATTGGGTTTGGTT	*Notropis buccula*
	LB	TAGTGGGCGGCTGAGGT	*Notropis buccula*

Analytical sensitivity (dilution-series detection) and lot-level QC criteria: Analytical sensitivity was evaluated using ten-fold serial dilutions of purified target DNA. The dilution series provided an estimate of the range of template concentrations over which each assay could reliably detect target DNA under controlled conditions. Detection through high dilution levels indicated that the assay could amplify low amounts of purified target DNA, while failure or delayed amplification near the lowest concentrations helped identify the practical limits of detection. These results were used to determine whether the assays were sufficiently sensitive to proceed to environmental sample testing. For pellet lot 101525, acceptance criteria required detection through 1:10,000 dilutions and absence of false positives among NTCs and designated cross-reactor DNA (Appendix I). Sensitivity and reporting of detection behavior near assay limits followed recommended best practices for environmental DNA assays (Klymus et al. 2020).

Analytical specificity and cross-reactivity screening: Analytical specificity was assessed using NTCs and a cross-reactor panel of non-target DNA. During optimization, reaction

temperature was used to improve specificity (e.g., cleaner performance for the *N. buccula* assay at 68 °C). In expanded screening, cross-reactivity was evaluated by comparing amplification behavior of cross-reactor DNA relative to positive-control DNA, with particular attention to delayed amplification in cross-reactors. Cross-reactivity testing was especially important because the focal species co-occur with other cyprinids that may be closely related or share conserved mitochondrial regions. Cross-reactor reactions were interpreted relative to positive-control amplification, with rapid amplification of non-target DNA considered a major specificity concern and substantially delayed amplification treated as potential low-level cross-reactivity, requiring cautious interpretation. This distinction was important for separating strong evidence of target detection from weak or late signals that may occur near assay limits.

Scope and development of a standard operating procedure for field testing: Field validation and implementation followed a standardized SOP for performing LAMP assays on environmental samples using Agdia's Amp1 extraction buffer and dilution into 25 mM Tris buffer (pH 8.3). We developed an SOP that covers unconcentrated water samples and water samples collected on filters, LAMP reaction setup, incubation, and basic data interpretation (summarized in Table 9). Reagents included Amp1 extraction buffer, 25 mM Tris buffer (pH 8.3), and a LAMP reaction mix (i.e., lyophilized LAMP pellets produced by Agdia). The extraction and dilution workflow was intentionally simple to support use under field conditions. Amp1 extraction buffer was used to release DNA from water or filter samples during a short room-temperature incubation, and subsequent dilution into Tris buffer helped reduce the influence of environmental inhibitors before amplification. This approach avoided the need for full laboratory DNA extraction during field screening while retaining a standardized template preparation step. Reactions were prepared, as described below, using 2 mL screw-cap transfer tubes with pre-measured Amp1 buffer.

Sample preparation for unconcentrated water (river water): Testing unconcentrated river water provided a rapid, minimal-equipment option for field screening. Although unconcentrated water may contain less target DNA than filtered samples, it reduces processing time and equipment needs, making it useful for situations where immediate, qualitative detection information is more valuable than maximizing DNA yield. For unconcentrated water samples, environmental water was mixed 1:1 (v:v) with Amp1 extraction buffer, vigorously shaken, and incubated for 5 minutes at room temperature. A 5 µL aliquot of the crude extract was then diluted into 100 µL of 25 mM Tris buffer (pH 8.3). The diluted extract was then used as the template to rehydrate LAMP reactions (e.g., 25 µL of diluted extract added to a lyophilized pellet) following the assay-specific protocol (see below).

Sample preparation for filtered samples: Filter-based testing was included because filtration concentrates DNA from a larger volume of water and should improve detection probability when target DNA concentrations are low or spatially patchy. Including both unconcentrated water and filter-based workflows allowed the SOP to support rapid screening as well as a more sensitive sample preparation option that could be conducted in the lab. For filtered samples, filters were placed in a sterile tube and sufficient Amp1 extraction buffer was added to fully submerge the filter (~1 mL). After a 5-minute room-temperature incubation, the extract was collected and diluted by adding 5 µL extract to 100 µL of 25 mM Tris buffer (pH 8.3). The diluted extract was then used to rehydrate LAMP reactions per the assay-specific protocol (see below).

Amplification conditions and interpretation: Agdia's AmpliFire isothermal fluorometer was used in the field using the species-specific reaction temperatures (either 67 °C or 68 °C) and

Process	Sample type	Extraction step	Dilution / template prep	Amplification & QC requirements
Sample preparation	Unconcentrated water	Mix water 1:1 with Amp1; 5 min RT	5 µL extract into 100 µL 25 mM Tris (pH 8.3)	Incubate 45 min. at 67–68 °C (species-specific); include controls
Sample preparation	Filtered water sample	Submerge filter in Amp1; 5 min RT	5 µL extract into 100 µL 25 mM Tris (pH 8.3)	Incubate 45 min. at 67–68 °C (species-specific); include controls
Controls & QA	All runs	Optional extraction blank	NTC and positive control prepared per protocol	Run invalid if amplification threshold was not reached in the 45-minute assay or if NTCs or positive control failed; document and repeat if needed.
Documentation	All runs			Record date, operator, sample ID/type, reaction conditions, temperature, time, and results for all controls and samples; document field conditions for each site sampled.

Table 9. Summary of field lamp procedures.

incubating reactions for ~45 minutes. A reaction was interpreted as positive when fluorescence crossed the instrument-defined threshold within the assay window (45 minutes) and the corresponding controls performed as expected. Reactions that produced weak, delayed, or borderline amplification were documented as ambiguous and repeated when possible.

Controls, quality assurance, and documentation: No-template controls (NTC), positive controls (diluted target species DNA extract), and extraction blanks were used to ensure assay effectiveness. Runs were considered invalid if amplification did not reach optimal thresholds within the timeframe of the 45-minute assay, or if controls did not perform as expected (NTC and extraction blank negative; positive control positive). Finally, detailed records were taken in a field notebook for each assay, including date, AmpliFire operator, sample ID/type, volumes and deviations, reaction conditions, incubation time, sample and control results, information on any reruns or issues, and field conditions.

LAMP and seining field validation: LAMP assays were conducted in the field by taking 8 equidistant samples (per species and site) along a 500-m reach for each site assessed, with replicate 1 (R1) taken at the bottom of the reach, replicate 8 (R8) taken at the top of the reach, and other replicates taken sequentially from downstream to upstream. Eight spatially distributed

LAMP samples were collected along each 500-m reach to account for the patchy distribution of fish and environmental DNA within flowing-water habitats. Sampling from downstream to upstream also reduced the chance that field crews would disturb upstream habitats before collection. This spatially replicated design allowed detection to be summarized not only at the site level, but also across downstream, middle, and upstream portions of each reach. A total of five sites were assessed two times (November and December of 2025). Sites were selected to span a range of expected detection probabilities based on prior sampling history, including locations where focal species had previously been detected at different apparent densities and locations where detections were expected to be less likely. Repeating assessments across November and December provided an opportunity to evaluate assay behavior across separate field events and environmental conditions.

During the December 2025 sampling event, seine hauls were concurrently taken at each site in order to corroborate positive LAMP detections. The seining method was to seine at least twice at each transect and continue seining until either A) both focal shiner species were observed, or B) no additional species were observed with a new seine haul. To compare detection performance between seining and LAMP for the two focal species, *Notropis buccula* and *Notropis oxyrhynchus*, detection data were summarized as binary outcomes (1 = detect, 0 = no detect) for each site, transect, and method. For the paired dataset, detections from the seining (Seine) and loop-mediated lyophilized amplification (LAMP) methods were compared across the downstream, middle, and upstream portions of each reach.

In total, 10 LAMP detections were observed across both species and all sampling events (Table 10). Most site × month combinations were entirely negative, but some positive replicates occurred for *N. buccula* at site 10 in November and site 21 in December, and for *N. oxyrhynchus* at sites 3, 10, and 18 in November and site 21 in December. The strongest LAMP signal occurred for *N. oxyrhynchus* at site 10 in November, where multiple replicates were positive, while most other site-month combinations had either 0% positivity or only a single positive replicate. Overall, LAMP detections were spatially restricted and intermittent, with relatively few site-month combinations showing amplification. Seining detected both shiner species more frequently than LAMP (Table 11). Seining yielded multiple detections across sites 10, 15, 18, and 21, whereas LAMP detections were restricted to site 21.

In sum, the LAMP component of this work 1) successfully produced species-specific, field-deployable LAMP assays for both focal shiner species; 2) established a reproducible in silico design and screening workflow; 3) transferred candidate assays to a commercial partner (Agdia) for optimization and lyophilized pellet formulation; and 4) developed a standardized SOP for field and laboratory implementation. Field validation demonstrated that the LAMP assays developed for this project could detect target DNA from environmental water samples taken under field conditions, but detections were less frequent and more spatially intermittent than detections from seining. This pattern is consistent with the expectation that early-stage, field validation of species-specific eDNA assays can be sensitive to sample volume, DNA concentration, flow conditions, inhibition, and the spatial distribution of target organisms. Thus, while our results support the feasibility of LAMP as a rapid, point-of-use detection tool, additional optimization of field sampling design, sample concentration, and replicate number are needed before LAMP should be used as a standalone basis for management decisions. In its current form, the assay is best viewed as a rapid screening tool that can complement seining, DNA metabarcoding, and other monitoring approaches for Sharpnose and Smalleye shiners in the Upper Brazos River.

Table 10. LAMP field validation results for *Notropis buccula* and *N. oxyrhynchus* detections from November and December 2025. R1-R8 are field replicates, with R1 sampled from water at the most downstream end of the reach and R8 sampled from water at the most upstream end of the reach. Detections are indicated by "1" and non-detections are indicated by "0". Seine detection data are available for associated seine hauls conducted in December. At site 18 in November, there was an instrument error (E), which prevented us from being able to acquire usable data.

Species	Month	Site	R1	R2	R3	R4	R5	R6	R7	R8	% pos. detections
Notropis buccula	Nov.	3	0	0	0	0	0	0	0	0	0
	Nov.	10	0	1	0	1	0	0	0	0	25
	Nov.	15	0	0	0	0	0	0	0	0	0
	Nov.	18	E	E	E	E	E	E	E	E	Run fail.
	Nov.	21	0	0	0	0	0	0	0	0	0
	Dec.	3	0	0	0	0	0	0	0	0	0
	Dec.	10	0	0	0	0	0	0	0	0	0
	Dec.	15	0	0	0	0	0	0	0	0	0
	Dec.	18	0	0	0	0	0	0	0	0	0
	Dec.	21	0	0	0	1	0	0	0	0	12.5
Notropis oxyrhynchus	Nov.	3	1	0	0	0	0	0	0	0	12.5
	Nov.	10	1	0	0	0	0	1	1	1	50
	Nov.	15	0	0	0	0	0	0	0	0	0
	Nov.	18	0	0	0	0	1	0	0	0	12.5
	Nov.	21	0	0	0	0	0	0	0	0	0
	Dec.	3	0	0	0	0	0	0	0	0	0
	Dec.	10	0	0	0	0	0	0	0	0	0
	Dec.	15	0	0	0	0	0	0	0	0	0
	Dec.	18	0	0	0	0	0	0	0	0	0
	Dec.	21	0	0	0	0	0	1	0	0	12.5

Table. 11. Summary of LAMP field validation results compared to concurrent seining events conducted in December, 2025. Detections are indicated by "1" and non-detections are indicated by "0". At each site, Transect 1 was the downstream-most transect, Transect 3 was the middle-most transect, and Transect 5 was the upstream-most transect.

Site	**Transect**	**Method**	***Not buc***	***Not oxy***
3	1	Seine	0	0
3	3	Seine	0	0
3	5	Seine	0	0
10	1	Seine	1	0
10	3	Seine	1	1
10	5	Seine	1	0
15	1	Seine	0	0
15	3	Seine	1	1
15	5	Seine	0	0
18	1	Seine	1	0
18	3	Seine	0	0
18	5	Seine	1	0
21	1	Seine	1	1
21	3	Seine	1	1
21	5	Seine	1	1
3	1	LAMP	0	0
3	3	LAMP	0	0
3	5	LAMP	0	0
10	1	LAMP	0	0
10	3	LAMP	0	0
10	5	LAMP	0	0
15	1	LAMP	0	0
15	3	LAMP	0	0
15	5	LAMP	0	0
18	1	LAMP	0	0
18	3	LAMP	0	0
18	5	LAMP	0	0
21	1	LAMP	0	0
21	3	LAMP	1	0
21	5	LAMP	0	1

Task 4: Agency will recommend efficient and effective survey methodologies for long-term ecological monitoring for the species of interest, co-occurring species, and habitat associations, incorporating practical considerations such as field conditions, cost, and equipment availability.

When coupled with instream environmental data, standardized seining was extremely useful for understanding environmental factors associated with differences in assemblage structure (Figures 4 and 5), estimating relative patterns of distribution and abundance of the focal shiners (Figures 14 and 15), quantifying threshold responses of Sharpnose and Smalleye shiners to key environmental gradients (Figures 7-10), and identification of high quality habitat conditions and the availability of such habitats in space and time (Figures 11-13). Compared with standardized seining, fyke nets and especially minnow traps greatly underrepresented species occurrences and relative abundances. Note that increasing the duration of deployment of fyke nets could possibly increase the number of individuals and species collected, however the selective nature of those methods is likely to persist, and increase in deployment time would also likely increase mortality. It is our opinion that extending passive sampling duration would be unreasonable from a logistics standpoint for standard biomonitoring procedures (requiring multiple site visits to deploy and recover nets/traps for a single species composition observation). eDNA metabarcoding and LAMP assays were unreliable at detecting the two target species. Specifically, when comparing eDNA metabarcoding to presence of each species from standardized seining we observed 76% and 57% false negative rates for Sharpnose and Smalleye shiners, respectively. In short, standardized seining results in a greater diversity of taxa collected, with verifiable presence (i.e. direct observation) and provides data on relative abundances of taxa, whereas all other methods tested greatly underestimate the presence of the focal species and other co-occuring taxa. In particular, data from eDNA metabarcoding, LAMP assays and minnow traps should be interpreted with caution. In addition to being unreliable from a detection standpoint due to the very high false negative rate, eDNA approaches do not provide estimates of relative abundance and lack direct verification. At best, such approaches can compliment the more robust direct observational data obtained from standardized seining, but still require compromises in certain analytical approaches (e.g. requires converting seine abundance to presence-absence data for combined use with eDNA presence-absence observations in species co-occurrence modeling).

Based on the results from our analyses, we recommend the standardized seining methods for fish assemblage surveys and habitat quantification used in this study as the basis for long-term ecological monitoring. This recommendation follows the TCEQ (2014) standard protocols for wadable streams. Monthly surveys provided the temporal resolution necessary to identify dynamics in environmental conditions and responses of the focal species to those dynamic conditions – seasonal surveys would be insufficient to capture environmental and population dynamics, especially in response to drought. In addition, higher temporal resolution data on dissolved oxygen concentration and temperature (i.e. diel quantification from sensors rather than point estimates at the time of sampling) is needed to understand where, when, and how long the target species are experiencing physiologically stressful conditions that can affect survivorship as well as sublethal impacts on growth and reproduction. Data on movement of individuals for reproduction and metapopulation functionality (e.g. recovery of local populations following drought, maintenance of genetic diversity) is needed, but additional research on longer-term

effects of PIT tagging is required before that approach is recommended to be applied as part of a biomonitoring program.

Although we made significant advances in the development of novel molecular approaches for biomonitoring Sharpnose and Smalleye shiners, namely the development and validation of a novel primer suitable for detection of the target species in eDNA metabarcoding and real-time field deployable LAMP assays for both species, our analyses comparing molecular approaches to traditional standardized seining indicate that false negatives in eDNA metabarcoding and LAMP assays make these methods unreliable, even with the methods we used to reduce inhibition (Figures 17 and 22, Table 9). The reality of the Upper Brazos River basin, especially during summer drought conditions, is that multiple environmental factors that degrade DNA or inhibit amplification are commonplace and expected to only increase over time. The prevalence of inhibitors meant that we were not able to identify specific conditions in which eDNA metabarcoding is most suitable for monitoring the focal shiner species – conditions where false negatives were observed were broadly overlapping with conditions where eDNA corroborated seine data (Figure 18). Additional research is needed to build on the foundations developed in this study to further refine the molecular approaches to increase detection probability and reduce likelihood of false negatives. While the initial focus of future studies should be on reducing or resolving the issue of false negatives via field and lab techniques to reduce inhibition, there were quite a few observations were eDNA detected one or both of the focal species but no individuals were collected by seining. Such non-validated positive detections should be investigated with more exhaustive (e.g. depletion) surveying to substantiate that such observations are not false positives, along with studies to estimate eDNA transport distance to better understand the relationship between location of detection and location of original eDNA source. Our species occupancy models demonstrate the utility of integrating data from seining and eDNA, but we are hesitant to recommend models based on eDNA samples alone, and integrating data from those methods requires using presence-absence data only.

Practical considerations such as field conditions, cost, and equipment availability do not alter our recommendation that biomonitoring for Sharpnose and Smalleye shiners be conducted using standardized seining and habitat quantification based on the TCEQ (2014) standard methods for wadable streams. Occasional high flows can prevent safe and effective seining, but also prevent the use of all other methods we compared. Even collection of water samples for eDNA applications is affected by high flows as water would only be collected from the margin (rather than the thalweg) and DNA transport rates, effects of increased turbidity, etc., would further complicate an already unreliable method. The passive sampling techniques (fyke nets and minnow traps) also are less suitable at very low or non-flowing conditions where seines are still highly efficient at surveying fish species composition and relative abundance. Equipment availability is only a significant concern for LAMP assays, but washing and sterilizing bottles, availability of dry ice for flash freezing samples, and facilities and expertise for sample storage and preparation are additional logistical burdens associated with eDNA approaches. A full cost-benefit analysis of the methods compared would be ill-advised given that the eDNA and other approaches were inherently unreliable and not suitable for any meaningful biomonitoring program for the focal species. This issue is exacerbated by the highly volatile nature of costs associated with travel, transport, personnel, equipment and sequencing. That said, all methods require repeated site visits by similarly sized crews of field technicians and habitat conditions should be quantified using the same methods. Beyond those base considerations, seines are comparatively common and cost-effective to use, store and replace if damaged. Training is

required for species identifications, but that is consistent with the other methodologies except for eDNA methods. eDNA methods require significant equipment/facilities and preparation by highly-trained personnel before, during and after surveys (e.g. bottle sterilization, sample storage, filtration, extraction, library preparation, high-throughput sequencing, bioinformatics). Ideally, data from all methods should be analyzed and interpreted by highly qualified personnel with expertise in the field, lab and analytical methods used as well as fish biology/ecology and highly dynamic plains river systems.

Task 5: Agency will upload all data and results from this project to a Comptroller-approved public data repository such as Figshare or Dryad.

All available data have gone through standard QA/QC procedures and are stored in multiple hardcopy and digital formats for long-term preservation. All analyses were conducted using 'working' datasets to retain the integrity of 'raw' preserved datasets. Project data are archived in FigShare (10.6084/m9.figshare.32080353), except for the metabarcoding raw reads which are archived in NCBI SRA (Project accession number: PRJNA1467177; Individual SRA submission numbers for 11 batches within the project: SUB16135481, SUB16192931, SUB16192946, SUB16192958, SUB16193023, SUB16193044, SUB16193061, SUB16193160, SUB16193200, SUB16193601, SUB16193624). Note that NCBI SRA does not allow files with no sequences – those samples without sequences are actual zero read samples (e.g. during high flow events) and are included in the bioinformatically processed dataset.

Literature Cited

Allan, H., P. Unmack, R.P. Duncan, and M. Lintermans. 2018. Potential impacts of PIT tagging on a critically endangered small-bodied fish: a trial on the surrogate Mountain Galaxias. Transactions of the American Fisheries Society 147: 1078-1084.

Anderson, K.A., T. L. Beitinger, and E.G. Zimmerman. 1983. Forage fish assemblages in the Brazos River upstream and downstream from Possum Kingdom Reservoir, Texas. Journal of Freshwater Ecology 2: 81-88.

Anderson, M. J. 2001. "A new method for non-parametric multivariate analysis of variance." Austral Ecology 26: 32–46.

Angeler, D. G., O. Viedma, and J. M. Moreno. 2009. "Statistical performance and information content of time lag analysis and redundancy analysis in time series modeling." Ecology 90: 3245–3257.

Auerbach, D.A., D.M. Merritt, and P.B. Shafroth. 2013. Tamarix, hydrology, and fluvial geomorphology. Tamarix: A Case Study of Ecological Change in the American West, Oxford University Press, UK: 99-122.

Baker, M.E., and R.S. King. 2010. A new method for detecting and interpreting biodiversity and ecological community thresholds. Methods in Ecology and Evolution 1: 25-37.

Baldys, S., and F.E. Schalla. 2012. Base flow (1966-2009) and streamflow gain and loss (2010) of the Brazos River from the New Mexico-Texas State line to Waco, Texas: US Geological Survey.

Bangs, B.L., M.R. Falcy, P.D. Scheerer, and S.Clements. 2013. Comparison of three methods for marking a small floodplain minnow. Animal Biotelemetry 1: 18.

Bolland, J.D., I.G. Cowx, and M.C. Lucas. 2009. Evaluation of VIE and PIT tagging methods for juvenile cyprinid fishes. Journal of Applied Ichthyology 25: 381-386.

Borcard, D., and P. Legendre. 2002. "All-scale spatial analysis of ecological data by means of principal coordinates of neighbour matrices." Ecological Modelling 153: 51–68.

Borcard, D., F. Gillet, and P. Legendre. 2018. Numerical Ecology with R. 2nd ed. Use R! series. Springer, Cham.

Brotherson, J.D., and D. Field. 1987. Tamarix: impacts of a successful weed. Rangelands Archives 9: 110-112.

Carim, K. J., Dysthe, J. C., Young, M. K., McKelvey, K. S., & Schwartz, M. K. (2016). An environmental DNA assay for detecting Arctic grayling in the upper Missouri River basin, North America. Conservation Genetics Resources, 8(3), 197–199.

Cary, J.B., J.L. Holbrook, M.E. Reed, T.B. Austin, M.S. Steffensen, S. Kim, K.C. Pregler, and Y. Kanno. 2017. Survival of upper piedmont stream fishes implanted with 8-mm passive integrated transponder tags. Transactions of the American Fisheries Society 146: 1223-1232.

Cross, F.B. 1953. A new minnow, Notropis bairdi buccula, from the Brazos River, Texas. The Texas Journal of Science 5: 252-259.

Dodds, W.K., W.H. Clements, K. Gido, R.H. Hilderbrand, and R.S. King. 2010. Thresholds, breakpoints, and nonlinearity in freshwaters as related to management. Journal of the North American Benthological Society 29: 988-997.

Durham, B.W. 2007. Reproductive ecology, habitat associations, and population dynamic of two imperiled cyprinids in a Great Plains river. PhD dissertation. Texas Tech University. 183 pp.

Durham, B.W. and G.R. Wilde. 2009. Population dynamics of the smalleye shiner, an imperiled cyprinid fish endemic to the Brazos River, Texas. Transactions of the American Fisheries Society 138: 666-674.

Fields, A. T., Conway, K. W., Dolan, E. P., Swift, D. G., Monroe, A. A., Hollenbeck, C. M., Bean, P. T., Anderson, J. D., & Portnoy, D. S. (2024). Complete mitochondrial genomes of Notropis oxyrhynchus and Notropis buccula (Cypriniformes: Leuciscidae). Mitochondrial DNA Part B: Resources, 9(11), 1569–1574.

Gelwick, F.P. and R.Y. Li. 2002. Mesohabitat use and community structure of Brazos River fishes in the vicinity of the proposed Allens Creek Reservoir. Final report to Texas Water Development Board for contract number 2001-483-376. 55 pp.

Goldberg, C. S., Turner, C. R., Deiner, K., Klymus, K. E., Thomsen, P. F., Murphy, M. A., Spear, S. F., McKee, A., Oyler-McCance, S. J., Cornman, R. S., Laramie, M. B., Mahon, A. R., Lance, R. F., Pilliod, D. S., Strickler, K. M., Waits, L. P., Fremier, A. K., Takahara, T., Herder, J. E., & Taberlet, P. (2016). Critical considerations for the application of environmental DNA methods to detect aquatic species. Methods in Ecology and Evolution, 7(11), 1299–1307.

Groffman, P.M., J.S. Baron, T. Blett, A.J. Gold, I. Goodman, L.H. Gunderson, B.M. Levinson, M.A. Palmer, H.W. Paerl, and G.D. Peterson. 2006. Ecological thresholds: the key to successful environmental management or an important concept with no practical application? Ecosystems 9: 1-13.

Hoagstrom, C.W. and T.F. Turner. 2013. Recruitment ecology of pelagic-broadcast spawning minnows: paradigms from the ocean advance science and conservation of an imperiled freshwater fauna. Fish and Fisheries 16: 282-299.

Kelly M. and G.R. Wilde. 2020. Effects of altered water quality on populations of Smalleye Shiner and Sharpnose Shiner in the upper Brazos River. Water Quality Technical Series Publication WQTS-2020-01. Texas Parks and Wildlife Department, Austin, TX. 63 pp.

Klymus, K. E., Merkes, C. M., Allison, M. J., Goldberg, C. S., Helbing, C. C., Hunter, M. E., Jackson, C. A., Lance, R. F., Mangan, A. M., Monroe, E. M., Piaggio, A. J., Stokdyk, J. P., Wilson, C. C., & Richter, C. A. (2020). Reporting the limits of detection and quantification for environmental DNA assays. Environmental DNA, 2(3), 271–282.

Legendre, P., and S. Legendre. 2012. Numerical ecology. Elsevier, Amsterdam.

Marks, D.E. 1999. Life history characteristics of the sharpnose shiner (Notropis oxyrhynchus) and the smalleye shiner (Notropis buccula) in the Brazos River, Texas. PhD dissertation. Texas Tech University. 97 pp.

Mayes, K.B., G.R. Wilde, M.E. McGarrity, B.D. Wolaver, and T.G. Caldwell. 2019. Watershed-scale conservation of native fishes in the Brazos River Basin, Texas. In American Fisheries Society Symposium, 315-343.

Moore, G.A. 1944. Notes on the early life history of Notropis girardi. Copeia 1944: 209-214.

Moss, R.E. and K.B. Mayes. 1993. Current status of Notropis buccula and Notropis oxyrhynchus in Texas. River Studies Report 8. Austin, TX. Texas Parks and Wildlife Department, 150 pp.

Nagamine, K., Hase, T., & Notomi, T. (2002). Accelerated reaction by loop-mediated isothermal amplification using loop primers. Molecular and Cellular Probes, 16(3), 223–229.

Notomi, T., Okayama, H., Masubuchi, H., Yonekawa, T., Watanabe, K., Amino, N., & Hase, T. (2000). Loop-mediated isothermal amplification of DNA. Nucleic Acids Research, 28(12), e63.

Oksanen, J., G. Simpson, F. Blanchet, R. Kindt, P. Legendre, et al. 2022. "_vegan: Community Ecology Package_. (Version 2.6-4) [R]"

Ostrand, K.G. 2000. Abiotic determinants of fish assemblage structure in the upper Brazos River, Texas. PhD dissertation. Texas Tech University. 115 pp.

Ostrand, K., and G. Wilde. 2002. Seasonal and spatial variation in a prairie stream-fish assemblage. Ecology of Freshwater Fish 11: 137-149.

Pennock, C.A. 2017. Effects of PIT tags on Red Shiner Cyprinella lutrensis and Sand Shiner Notropis stramineus. Transactions of the Kansas Academy of Science 120: 87-93.

Pennock, C.A., and L.A. Bruckerhoff. 2020. Qualitative observations of successful spawning by two species of small-bodied minnows following PIT tagging. Western North American Naturalist 80: 253-256.

Perkin, J.S., K.B. Gido, A R. Cooper, T.F. Turner, M.J. Osborne, E.R. Johnson and K.B. Mayes. 2015. Fragmentation and dewatering transform Great Plains stream fish communities. Ecological Monographs 85: 73–92.

Platania, S.P. and C.S. Altenbach. 1998. Reproductive strategies and egg types of seven Rio Grande cyprinids. Copeia 1998: 559-569.

Shafroth, P.B., J.R. Cleverly, T.L. Dudley, J.P. Taylor, C. VAN Riper III, E.P. Weeks, and J.N. Stuart. 2005. Control of Tamarix in the western United States: implications for water salvage, wildlife use, and riparian restoration. Environmental management 35: 231-246.

Schumann, D.A., K.N. Graeb, M.D. Wagner, B.D.S. Graeb, E. Prenosil, and J. Hoekwater. Suitability of surgically implanted 8-mm passive integrated transponder tags for small-bodied fishes. Journal of Applied Ichthyology 36: 682-692.

Schumann, D.A., M.E. Colvin, R.L. Campbell, M.D. Wagner, and D.E. Schwarz. 2021. Suitability of passive integrated transponder tags and a new monitoring technique for at-risk madtoms (Noturus spp.). Endangered Species Research 44: 1-10.

Texas Commission on Environmental Quality (TCEQ). 2014. "Surface Water Quality Monitoring Procedures, Volume 2: Methods for Collecting and Analyzing Biological Assemblage and Habitat Data." Texas Commission on Environmental Quality, Austin, TX.

Tiffan, K.F., I.G. Jezorek, and R.W. Perry. 2019. A field evaluation of the growth and survival of age-0 Oncorhynchus mykiss tagged with 8-mm passive integrated transponder (PIT) tags. Animal Biotelemetry 7: 9.

U.S. Fish and Wildlife Service (USFWS). 2014a. Endangered and threatened wildlife and plants; designation of critical habitat for the Sharpnose Shiner and Smalleye Shiner; final rule. Federal Register 79:149(4 August 2014):45242–45271.

U.S. Fish and Wildlife Service (USFWS). 2014b. Species status assessment report for the Sharpnose Shiner (Notropis oxyrhynchus) and Smalleye Shiner (N. buccula). USFWS, Ecological Services Field Office, Arlington, Texas.

U.S. Fish and Wildlife Service (USFWS). 2015. Recovery outline for Sharpnose Shiner and Smalleye Shiner. USFWS, Ecological Services Field Office, Arlington, Texas.

U.S. Fish and Wildlife Service (USFWS). 2018. Species Status Assessment Report for the Sharpnose Shiner (Notropis oxyrhynchus) and Smalleye Shiner (N. buccula) Version 2. Arlington Ecological Services Field Office, Arlington, Texas. 111 pp.

U.S. Fish and Wildlife Service (USFWS). 2020. Draft recovery plan for the sharpnose (Notropis oxyrhynchus) and smalleye (N. buccula) shiner. U.S. Fish and Wildlife Service Arlington, Texas.

Valsecchi, E., Bylemans, J., Goodman, S. J., Lombardi, R., Carr, I., Castellano, L., Galimberti, A., & Galli, P. (2020). Novel universal primers for metabarcoding environmental DNA surveys of marine mammals and other marine vertebrates. Environmental DNA, 2(4), e72.

Wilde, G.R. 2015. Reproductive Ecology and Population Dynamics of Fishes in the Upper Brazos River. State Wildlife Grant report to Texas Parks and Wildlife Department. 52 pp.

Wilde, G.R. and B.W. Durham. 2008. Daily survival rates for juveniles of six Great Plains cyprinid species. Transactions of the American Fisheries Society 137: 830-833.

Wilde, G. R., and A. C. Urbanczyk. 2013. Relationship between river fragment length and persistence of two imperiled Great Plains cyprinids. Journal of Freshwater Ecology 28: 445-451.

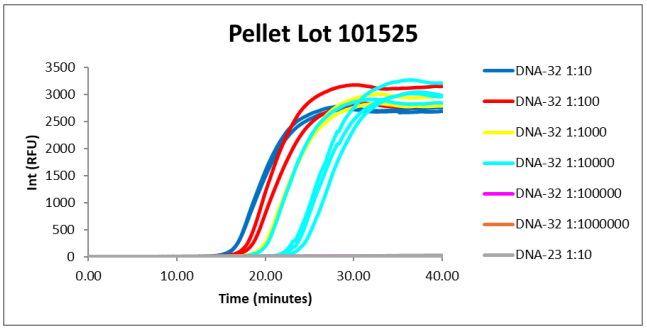
Zeug, S.C., K.O. Winemiller and S. Tarim. 2005. Response of Brazos River oxbow fish assemblages to patterns of hydrologic connectivity and environmental variability. Transactions of the American Fisheries Society 134: 1389-1399.

Appendix I. Quality control sheets for pelletized LAMP assays developed by Agdia for Sharpnose and Smalleye shiners (on subsequent, separate pages).

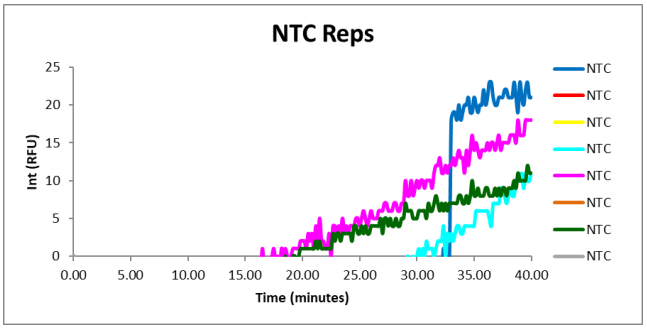
R&D Quality Control Report (Research Use Only) **Pellet Lot: 101525**

Test: *Notropis oxyrhynchus LAMP*
Acronym: Oxyrhynchus
Catalog Number: RDCS03
Format: AmplifyRP XRT

Sample	Dilution	Result
DNA-32	1:10	+,+
DNA-32	1:100	+,+
DNA-32	1:1000	+,+
DNA-32	1:10,000	+,+,+,+
DNA-32	1:100,000	-,-
DNA-32	1:1,000,000	-,-
DNA-23	1:10	-,-



Tube	Sample	Sample	Result
1	Water	N/A	-
2	Water	N/A	-
3	Water	N/A	-
4	Water	N/A	-
5	Water	N/A	-
6	Water	N/A	-
7	Water	N/A	-
8	Water	N/A	-



Performance Requirement: All detection down to 1:10,000 is required, matching all previously produced pellet lots and no false positives from no template controls (NTCs) and cross reactor DNA (23).

Protocol:

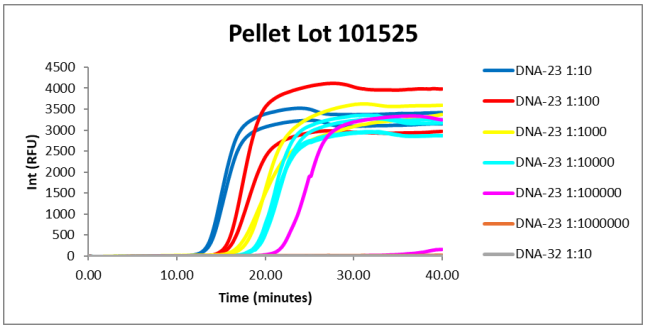
Sample: DNA is diluted serially in water and pellets are warmed to room temperature.
Diluent: 5µl of the sample is added to 100µL pre-dispensed 25mM tris buffer (PD2) and mixed.
Pellet: 25µl of the PD2/sample mixture is added to rehydrate the pellet and mixed.
Reaction: Reactions run for 40 minutes at 67°C and FAM measured using the AmpliFire.

R&D Scientist: X _____
Bryant Davenport, Lead Molecular Scientist

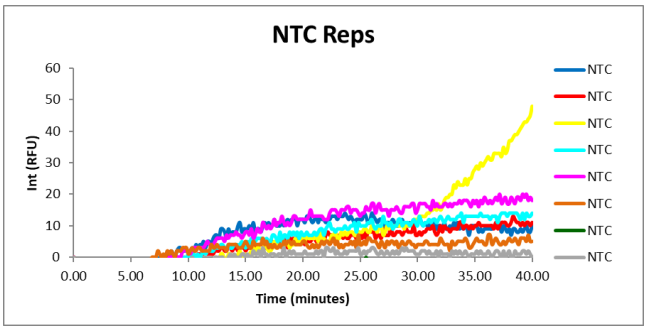
R&D Quality Control Report (Research Use Only) **Pellet Lot: 101525**

Test: *Notropis buccula LAMP*
Acronym: Buccula
Catalog Number: RDCS03
Format: AmplifyRP XRT

Sample	Dilution	Result
DNA-23	1:10	+,+
DNA-23	1:100	+,+
DNA-23	1:1000	+,+
DNA-23	1:10,000	+,+,+,+
DNA-23	1:100,000	+,-
DNA-23	1:1,000,000	-,-
DNA-32	1:10	-,-



Tube	Sample	Sample	Result
1	Water	N/A	-
2	Water	N/A	-
3	Water	N/A	-
4	Water	N/A	-
5	Water	N/A	-
6	Water	N/A	-
7	Water	N/A	-
8	Water	N/A	-



Performance Requirement: All detection down to 1:10,000 is required, matching all previously produced pellet lots and no false positives from no template controls (NTCs) and cross reactor DNA (32).

Protocol:

Sample: DNA is diluted serially in water and pellets are warmed to room temperature.
Diluent: 5µl of the sample is added to 100µL pre-dispensed 25mM tris buffer (PD2) and mixed.
Pellet: 25µl of the PD2/sample mixture is added to rehydrate the pellet and mixed.
Reaction: Reactions run for 40 minutes at 68°C and FAM measured using the AmpliFire.

R&D Scientist: X _____
Bryant Davenport, Lead Molecular Scientist